UPSCALE SYNTHESIS OF SYMMETRICAL AND UNSYMMETRICAL

MONOMERS TOWARDS BRIDGE TRIFLUOROMETHYLATED POLY (p-

PHENYLENEVINYLENE) AND THEORETICAL NMR STUDIES

By: JEAN PIERRE PINTO

A thesis submitted to the

Graduate School Camden

Rutgers, The State University

in partial fulfillment of the requirements

for the degree of

Master of Science Graduate Program in Chemistry

Written under the direction of

Dr. Alex J. Roche

And approved by

_____

Dr. Alex J. Roche

_____

Dr. Georgia Arbuckle-Keil

_____

Dr. Luke A. Burke

Camden, NJ

May 22, 2008

ABSTRACT OF THESIS

Upscale synthesis of symmetrical and unsymmetrical monomers towards bridge

trifluoromethylated poly (*p*-phenylenevinylene) and theoretical NMR studies

By: JEAN PIERRE PINTO

Thesis Director:

Dr. Alex J. Roche

The objective of this research is to up scale the synthesis of previously reported

symmetrical and unsymmetrical trifluoromethylated monomers in sufficiently high

amounts for the synthesis and characterization of bridge substituted poly (*p*-phenylene)

vinylene polymers. Theoretical NMR calculations are also made to differentiate between

diastereomers produced during synthesis. The preliminary polymerization reactions

yielded optimistic results but insufficient material was used for proper polymerization,

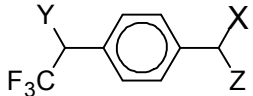characterization, and isolation. The monomers prepared are shown in Table 1:

	Y	X	Z
13	Cl	Cl	H
14	Cl	Cl	CF_3
15	Cl	$SC(S)OC_2H_5$	H
16	$OC(S)SCH_3$	$OC(S)SCH_3$	CF_3
17	$OC(S)SCH_3$	$OC(S)SCH_3$	H
18	Cl	$S(O)C_8H_{17}$	H
19	Cl	$S(O_2)C_8H_{17}$	H
20	OTos	OTos	H
22	OTos	OTos	CF_3
23	OTos	$SC(S)OC_2H_5$	H
24	OTos	$S(O)C_8H_{17}$	H
25	OTos	$S(O_2)C_8H_{17}$	H
26	$Py^+ CF_3SO_3^-$	$Py^+ CF_3SO_3^-$	CF_3
27	$Py^+ CF_3SO_3^-$	$Py^+ CF_3SO_3^-$	H

Table 1: Synthesized Monomers

Dedications

I dedicate this to my parents Dora and Jose Pinto and my sister Karina for their undying

love and support.

Acknowledgments

I would like to give my greatest thanks to my parents, Dora and Jose Pinto, for giving me the opportunity they never had and my sister Karina for her undying support. Thanks to my grandfather for having given his grandkids the opportunity of a lifetime. Special thanks to my best friends Jeanette, Joyce, Julio, Samad, and Hamal Patel for their support and friendship.

Thanks to Dr. Burke for being a committee member and part of my undergraduate and graduate education. Thanks to Dr. Maslen for being available whenever I needed him and for being part of my undergraduate and graduate education. Thanks to Dr. Georgia Arbuckle-Keil for being a committee member and also a part of my graduate education.

Finally, special thanks to Dr. Alex Roche my research advisor and professor for granting me the opportunity to join his research group and being the majority of my graduate and undergraduate education and expanding my deep interest in organic chemistry. I am inspired to want to continue my education in chemistry and gain ever more knowledge.

Table of Contents

List of Tables

List of Figures

List of Schemes:

Chapter 1: Introduction

Conductivity

Conduction is a physical property that is mostly associated with metals, but in recent decades this property has been exploited to be expanded into the realm of organic materials such as polymers. The most common model for conduction is the band model which extends the idea of a single bond between two atoms over a whole crystal structure.[1] In molecular orbital theory, when two identical atoms with a single electron are brought close enough together for their orbitals to overlap, two new orbitals are produced, one of lower energy and one of higher energy. The difference in energy levels is given by how strongly the two incoming orbitals overlap with one another. The two electrons will go in the lower energy state molecular orbital called the bonding orbital while the higher energy orbital called the anti-bonding orbital will remain vacant as shown in Figure 1:
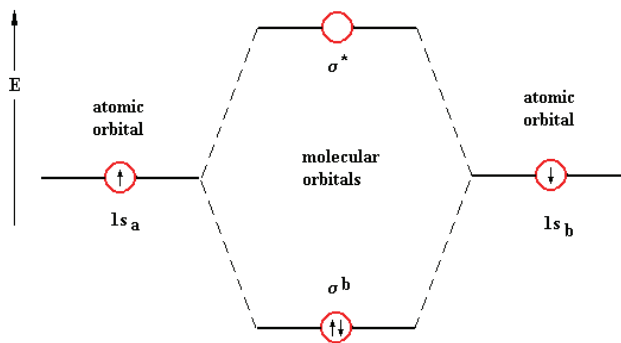
Energy level diagram for H_2 molecule formed from H_a and H_b atoms.

Figure 1: Energy Level Diagram for H_2

This model for two atoms may be extended to a crystal structure containing N ($\sim 10^{23}$) number of atoms. The overlap of N atoms produces N/2 low energy orbitals and N/2 higher energy orbitals; the new orbitals that are produced are all closely packed in

energy that they form a continuous "band". The electrons are considered to be delocalized, meaning they can take on any energy they would like. The lower energy band is called the bonding or valence band because it is completely filled. The higher energy band is called the anti-bonding or conduction band and remains vacant.
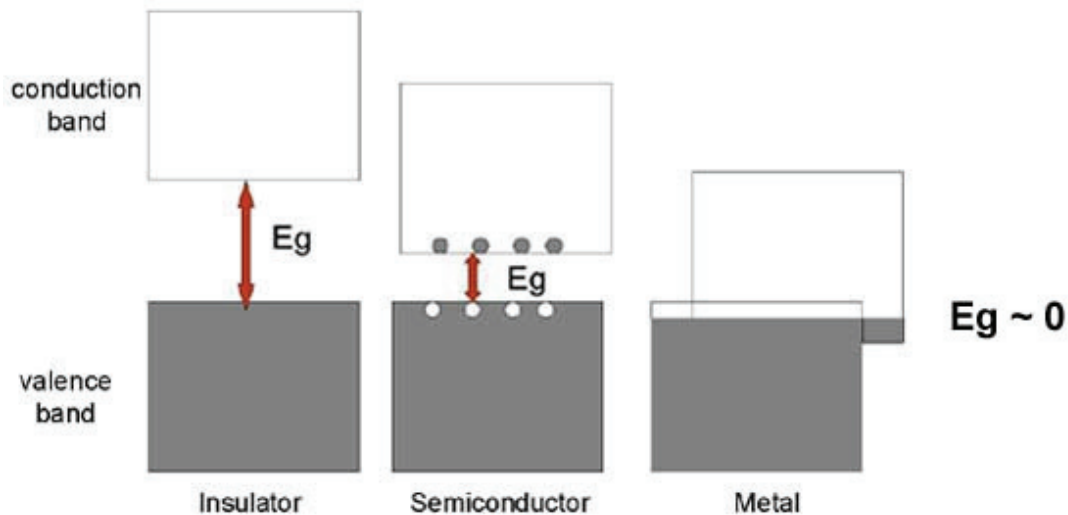
Figure 2: Energy Level Diagram for Metal, Semiconductor, and Insulator

The conductivity of a solid is determined by the occupation or vacancy of the energy bands and the magnitude of the energy gap (E_g) between them. As shown in Figure 2, in metals there is no band gap and therefore the electrons are able to move freely for conduction. In a semi-conductor the band gap is small and the electrons can be thermally excited across it and placing electrons into the conduction band. This process leaves holes in the valence band which are then also available for conduction. An insulator has a large band gap and the electrons cannot be thermally excited. E_g stands for the band gap energy and is given in units of eV(electron volts).

The conductivity of a solid is also dependent on temperature. In a metal all the electrons are available for conduction so the conductivity is determined by mobility. As

temperature is increased, the atoms within a crystal structure vibrate and interact with the electrons to scatter them. Therefore, in a metal the conductivity decreases as the temperature is increased. The same scenario holds true for semi-conductors, but the concentration of the charge carriers is much more temperature dependent than mobility, this is the dominating factor and so conductivity increases with increasing temperature. In an insulator the band gap is so large that it is difficult to thermally excite electrons and so conductivity remains low.

Polyacetylene

Polyacetylene is the prototype of conducting polymers and the simplest of all polymers only containing carbon and hydrogen atoms. Polyacetylene was first synthesized in 1955 by Natta et al. using the coordination catalyst system to polymerize ethylene and propylene.[2] Since then many investigations were brought to optimize synthesis and characterization. In the 1970's, MacDiarmid, Heeger, and Shirakawa at the University of Pennsylvania improved the synthetic route of polyacetylene and characterized the material. The work done to investigate the properties of polyacetylene established it as the first semi conducting and metallic organic polymer.[3]

Polyacetylene has two energetically nonequivalent structures which are shown below:
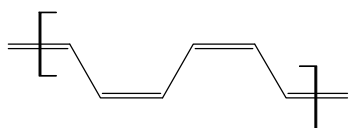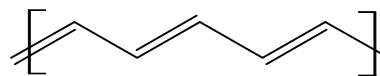
Cis-polyacetylene   Trans-polyacetylene

Figure 3: Cis and Trans Polyacetylene Structures

The cis-polyacetylene isomer is produced at low temperatures when acetylene is polymerized; the trans isomer is produced at higher temperatures beyond those used to initiate polymerization or when the cis isomer is introduced to elevated temperatures.[3]

Cis- and trans-polyacetylenes are intrinsic semi-conductors at room temperature with conductivities of 10^{-10} and 10^{-5} $Ohm^{-1}cm^{-1}$, respectively.[3] The conductivity of a material can be enhanced through various means by adding chemical impurities or electrochemically. There are two types of doping named p-doping and n-doping, which involve removing and adding impurities to create positive or negatively charged species, respectively. The most common p-dopants used are salts containing oxidizing cations such as NO_2^+, NO^+, Ag^+, and Fe^{3+}. The most common n-type dopants are the alkali metals such as Li, Na, and K. Electrochemical doping is also widely used by performing an electrolysis on various salt solutions such as KI, $Bu_4N^+ClO_4^-$, and $(n\text{-}Pr)_3\ NH^+AsF_6^-$. Investigations into the conductive properties of polyacetylene have shown dramatic effects upon chemical or electrochemical doping summarized in the tables below taken from reference 4. The superscripted letters a-f on Tables 2 and 3 are indicative of several things such as a specific type of doping, determination of composition, or determination of conductivity.

Table2 removed due to COPYRIGHT

Table 2: Common p-type dopants for Polyacetylene[4]

Table 3 removed due to COPYRIGHT.

Table 3: Common n-type dopants for Polyacetylene[4]

Photo Physics of Conducting Organic Polymers

Conducting organic polymers are primarily described by chemists as a

conjugation of overlapping π-orbitals which analogously make up the valence and

conduction bands in other solids. The gaps in the undoped material are small such that the absorption edge lies between the visible or near infrared region. The illumination of a polymer sample with light past the absorption edge results in excitation of a variety of particles discussed below. The three entities that are formed upon illumination are polarons, bipolarons, and solitons.

Polarons require that the electron which has been removed and the hole that is formed because of this are separated sufficiently so that they do not interact to form an exciton. This can occur by the electron and hole, within femtoseconds of creation, separating onto different chains. According to the SSH Hamiltonian,[5] polarons create two energy levels that are located symmetrically at the center of the band gap. The location relative to the edge of the valence or conduction band is determined by the chain length. In the case where the conjugation length is larger than the deformation, studies done by H.A. Mizes and E.M. Conwell on poly (p-phenylenevinylene) (PPV) indicate that the energy levels are between 0.15eV or 0.2eV from the nearest band edge.[5]

A bipolaron consists of two like charges with opposite spins bound together within the same conjugation length. Studies done on PPV indicate that two peaks in the absorption of the photo generated entities behaved similar with respect to intensity, temperature, and frequency dependence. The production of two similar peaks suggests that it is due to the presence of a bipolaron.[5]

The trans isomer of polyacetylene may exist as another isomer in which the double bonds are pointing down as opposed to up going from left to right. These two isomers are degenerate and this special feature of polyacetylene gives rise to a special kind of defect or excitation, the soliton or the antisoliton. A soliton or antisoliton is a

portion of chain or a domain wall separating two regions of different bond alternation. Apart from bond location, solitons and antisolitons have the same properties. Solitons exist as either neutral entities with spin ½ or as positive or negative species with spin 0. The existence of solitons is given by studies on undoped trans-polyacetylene using ESR; studies show the presence of about 1 spin per 1000 to 3000 atoms.[6]

PPV and PPV Derivatives

Many polymers and their derivatives have been studied since the synthesis of polyacetylene, but much attention has been paid to poly para-(phenylenevinylene) (PPV) and its derivatives due to their possible applications as light emitters due to their property of electroluminescence.[7,8] The property of electroluminescence gives PPV and its derivatives to be applicable as light emitting diodes(LED's) or organic light emitting diodes(OLED's). [9-12] There have been several PPV and PPV derivatives synthesized with varying side chains and lengths. Oligo(*p*-PPVs) and polymeric derivatives containing butyl, octyl, and dodecyl side groups have been synthesized by C. Xue, H.C. Lin and colleagues.[13,14] Extensive work has been done on the electron withdrawing effects of the cyano, CN, and trifluoromethyl group on the electronic and physical properties of PPV derivatives.[15] Samal et. al. calculated photoluminescence quantum efficiency (PQE) for several thin films of conjugated polymers such as PPV, (poly[2-methoxy-5-(2'-ethyl-hexyloxy)-1,4-phenylene vinylene]) MEH-PPV, and CN-PPV which is actually the cyano modified MEH given the name poly[2-Methoxy-5-(2'-ethylhexyloxy)-1,4-(1-cyanovinylene)phenylene]. An important note to take is that the measurements vary depending on many factors including type of casting, solvent used, and thickness of the

film amongst others. The measurement of PQE is important in order to determine how efficient the material will be in electronic devices. Their study showed that the PQE measurements for PPV, MEH-PPV, and CN-PPV are 0.07, 0.24, and 0.17, respectively.[15] Tilmann and Horhold[16] synthesized and performed physical characterization on two segmented PPV derivatives which contained cyano modified DSB(distyrylbenzene) segments. The following structural motif is presented in their article:
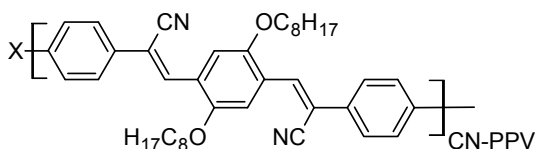
A: X= O **B**: X= O(CH$_2$)O

Figure 4: Cyano modified DSB

Their calculations for compound A in Figure 4 showed a band gap decrease from 2.79 eV to 2.46 eV, and the redox behavior is shifted to more positive values both in solution and as a solid film (E^{ox} 1.45 V, E^{red} -1.25 V) indicating high electron affinity.[16]

Some experimental results on doped and processed films have also been studied by Yongfang Li and colleagues.[17] The doping potentials of several PPV derivatives and most importantly MEH-PPV and CN-PPV which differ only by the placement of a cyano group on the ethylene linkage were measured by cyclovoltammetry. There are significant changes in all the measurements due to the placement of the strong electron withdrawing cyano group. The p-doping and n-doping potentials for MEH-PPV compared to CN-PPV were 0.68 and -1.49 for MEH-PPV versus 1.24 and -0.90 for CN-PPV. This indicates that CN-PPV is much more electronegative compared to MEH-PPV. The energy levels for these two compounds were also calculated. The energy levels for the HOMO and LUMO for MEH-PPV were -5.07 eV and -2.90 eV, respectively and the energy levels for the

HOMO and LUMO of the CN-PPV derivative were -5.63 and -3.49, respectively. The addition of an electron withdrawing group decreases the energy of both the HOMO and LUMO significantly. The energy band gaps were also measured and reported to be 2.17 and 2.14 eV for MEH-PPV and CN-PPV, respectively. The electrochemical properties of MEH-PPV and CN-PPV have been shown to function as a bulk donor/acceptor material. The photoluminescence and electroluminescence of the two polymers are quenched in the composite while the photosensitivity is enhanced. These effects are due to the charge transfer from the donor to acceptor and charge separation after photo excitation. This composite serves as a good candidate for use in light emitting diodes (LED's) with a photovoltaic efficiency and energy conversion efficiency that is 25 times larger than in diodes with only MEH-PPV alone and 100 times larger than in diodes made with CN-PPV.[16] Electro absorption studies of the cyano PPV derivatives have also been studied by Samal and his value of 2.6 eV agrees well with other studies.[18]

The trifluoromethyl group has also been incorporated in some PPV derivatives and studies have also been done on the electrochemical properties of these derivatives. Studies done by Vijila and colleagues on the charge mobility characteristics on some biphenyl substituted PPV derivates have incorporated the fluorine atom and trifluoromethyl group.[19] The proposed structure for their PPV derivatives with varying substituents which they label as PPVD1, PPVD2, PPVD3, and PPVD4 is given below:
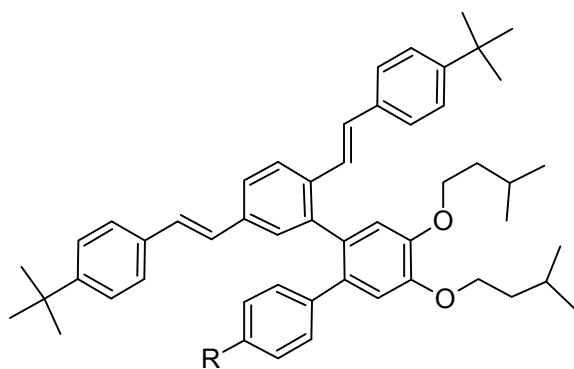
R= CF$_3$ PPVD1

OMe   PPVD2

F   PPVD3

H   PPVD4

Figure 5: Biphenyl substituted PPV derivative

The HOMO and LUMO energy levels were measured using cyclic voltammetry and found to be -5.59, -5.38, -5.52, and -5.47 eV for PPVD1, PPVD2, PPVD3, and PPVD4; the corresponding LUMO energy levels were -3.24, -3.03, -3.17, and -3.12. Due to the presence of the electron withdrawing effects of the CF$_3$ and F groups, PPVD1 and PPVD3 analogously show the lowest HOMO and LUMO energy levels. Charge mobility measurements were also made and shown to decrease with increase in substituent size from H, F, OMe, and CF$_3$. CF$_3$ PPV oligomers and polymers were studied for use as hole blocking layers in LEDs. Cyclovoltammetry studies on casted films showed a reduction potential of -1.3 eV which indicates it is easier to reduce compared to the CN analogue.[20]

Several mechanistic studies have also been done on the polymerization of PPV and its derivatives. The mechanism for the polymerization depends on the method of synthesis, the pre-cursor route such as the sulphinyl route[21] or the Gilch approach.[22] The pre-cursor approach depends on the preparation of a soluble pre-cursor polymer which

can be cast into thin films, while the Gilch approach involves the polymerization of 1,4-bis(halomethyl)-benzene monomers. The following scheme has been proposed by Issaris and colleagues:[23]
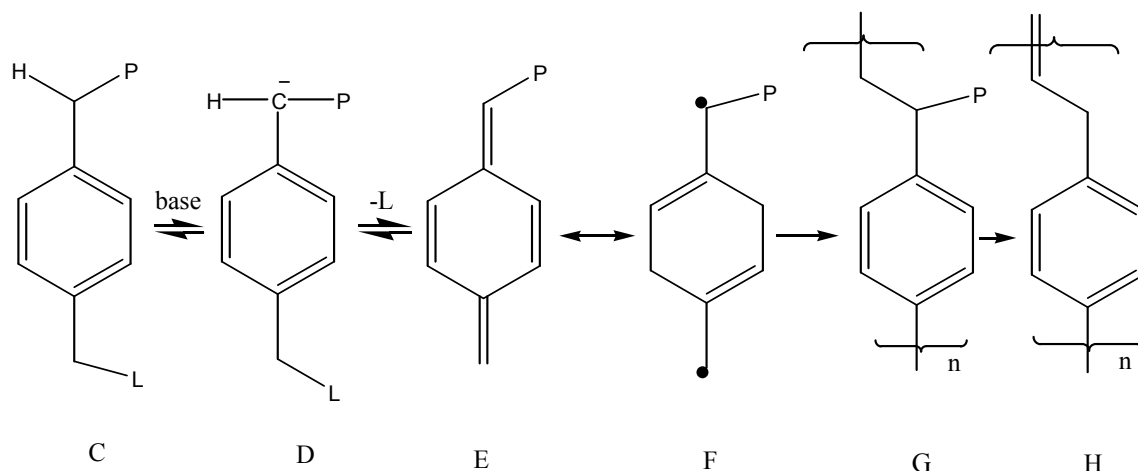
Scheme 1: PPV Mechanistic Route

Structure C must include a polarizer, P, because it stabilizes the anion formed in the acid-base equilibrium after deprotonation, and a leaving group, L, must also be present in order to form the p-quinodimethane intermediate, structure E. An important note is that the leaving group and/or polarizer need not be the same entity. The mechanism for the formation of structure E from structures C and D is an E_{1cb} (E1 conjugate base) type mechanism. From structure E the precursor polymer, G, is formed via a self initiating radical, F. The other mechanism that has been proposed is the nucleophilic scheme as depicted below:[24]
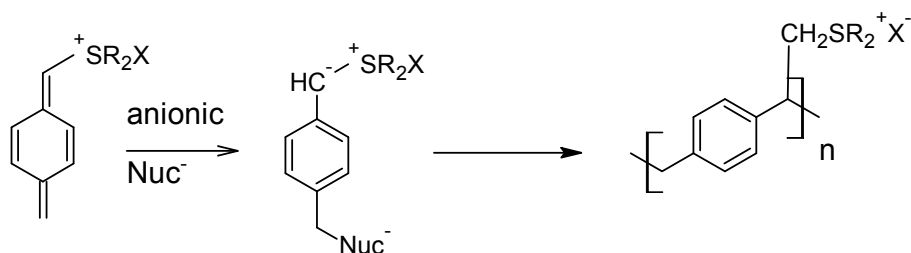
Scheme 2: Nucleophilic Mechanistic Route

Adriaensens and his fellow colleagues[25] have studied electron-poor and electron rich poly{[1,4-phenylene]-[1-(n-alkylsulfinyl)ethylene]}polymerizations via the sulfinyl route with varying leaving groups, solvents, and polarizers to further study these two possible mechanisms. The following table shows the different leaving groups and substituents used in their experiment:
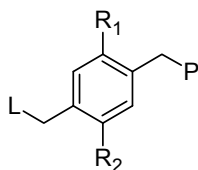
	L	$R_{1,2}$	P(polarizer S(O)R_3)
1	Cl	H	n-Butyl
2	I	H	n-Butyl
3	Cl	H	n-Octyl
4	Cl	CH_3	n-Butyl
5	Cl	CH_3	n-Octyl
6	Cl	OCH_3	n-Butyl
7	Br	Cl	n-Octyl
8	H	H	n-Octyl

Table 4: Disubstituted PPV Monomer Derivatives

Although it is very difficult to go into exact detail concerning the true mechanism of the polymerization, they did conclude several important points. The leaving group ability and substituent affects also play a major role. Electron donor substituents seem to enhance the formation of the *p*-quinodimethane system. The anionic mechanism is promoted by

electron withdrawing substituents. There is competition for formation of either high

molecular or low molecular weight polymers depending on the factors mentioned above.

A study[26] has shown that the synthesis of polymers can be controlled depending on

solvent scheme used. Through the use of NaH as a base and THF as a solvent, only low

molecular weight oligomers were obtained. When a more polar, aprotic solvent was used

the molecular weight increased tremendously. The GPC(gel permeation chromotagraphy)

trace reports a value of MW=3,000,000) for the synthesis of the sulfonyl n-butyl

derivative in DMF with NaH after 1 hour.

Organic Conducting Polymers and Their Applications

Organic polymers are considered polymers which contain carbon and hydrogen

and sometimes contain heteroatoms such as oxygen or sulfur. Upon the discovery and

synthesis of polyacetylene by MacDiarmid, Heeger, and Shirakawa, the field of

conducting polymers and their derivatives have received a great deal of attention for their

uses in applications. One researched aspect of conducting polymers is its use in

applications which require photoconduction such as LED's and OLED's.[27]

Chapter 2: Monomer Synthesis

Introduction

  All the compounds were synthesized, isolated, characterized, and reported by Dr. Alex Roche, Anne D. Loyle, and Jean Pierre Pinto in the Journal of Fluorine Chemistry.[28] The first synthetic step was to add the trifluoromethyl (CF_3) group onto either one or both benzylic positions. There are three synthetic approaches to introduce a CF_3 group which include using radicals, electrophilic addition, or nucleophilic addition.[29] There are many ways to produce the very electrophilic CF_3 radical which add themselves to electron rich aromatics. The disadvantages of using this synthetic route are the low yields, low stereo control, and the inability to do polytrifluoromethylations. Electrophilic trifluoromethylation never came to a rise and the only interesting aspect of this synthetic route was the production of some special salts synthesized by Umemoto.[30] Electrophilic trifluoromethylation is believed to have significant radical character; the difficulty in producing the CF_3^+ group as a stable entity along with the progress of other synthetic routes caused this synthetic route as a possibility. The most revolutionary method in the production and addition of a trifluoromethyl group into an organic molecule came from Ruppert in 1984.[31] The discovery and production of (trifluoromethyl) trimethylsilane CF_3-TMS was subsequently applied to various systems by Prakash.[32,33] The mechanistic scheme is explained in the figure below.
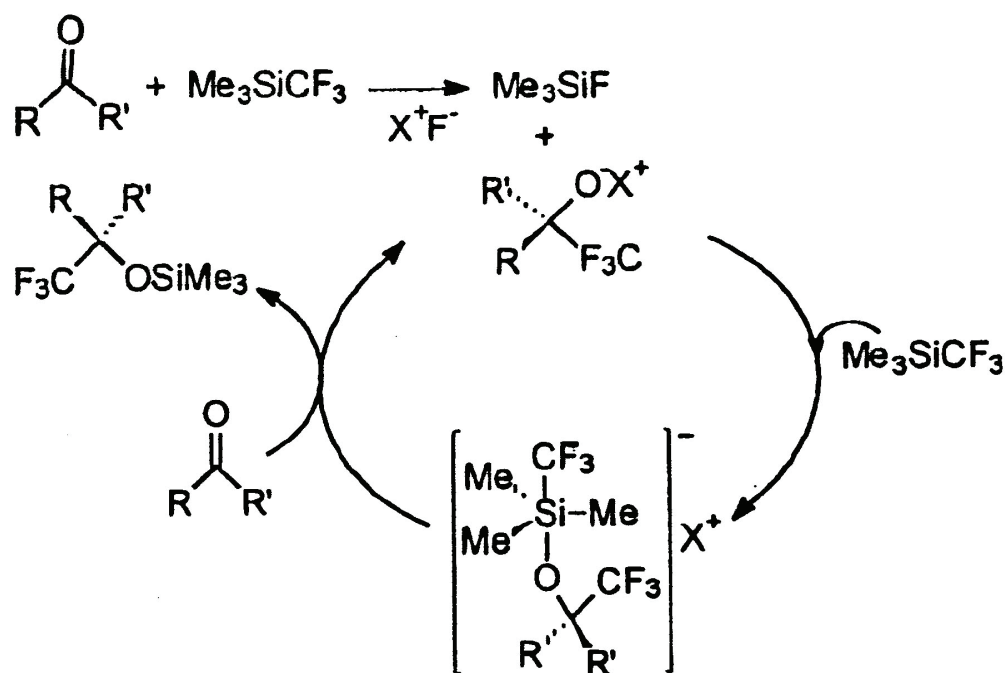
Figure 6: Nucleophilic Trifluoromethylation Mechanism

Any organic system which is electrophilic in nature such as a carbonyl may be used to introduce a CF_3 group. A catalytic amount of fluoride ion, usually donated by the compound tetrabutylammonium fluoride (TBAF), begins the process and the reaction is autocatalytic as each oxyanion is produced to carry on the reaction as seen in Figure 6. Research performed by Adams and colleagues experimentally proved that the reaction between TBAF and CF_3-TMS in acetonitrile forms a pentacoordinate silicon species, which serves as a source of fluoride ion or cyanomethyl cation, depending on the substrate.[34] There are several methods of using Ruppert's reagent in combination with various solvent schemes and fluoride sources. As reported by Mizuta and colleagues, they introduced a more convenient method by using potassium fluoride as a source for fluoride ions in varying solvent schemes, ammonium salts, and temperature ranges.[35]

Ruppert's reagent can be used to incorporate the trifluoromethyl group onto electrophilic carbon centers in systems such as ketones,[36] aldehydes, and imines amongst other systems.

Synthesis of Bis-CF$_3$ and Mono-CF$_3$ Diols

The synthesis of the diols began with a nucleophilic trifluoromethylation of compound 9, terephthaldicarboxaldehyde, in a solution of anhydrous THF; the reaction was successful and compounds 10 and 11 were formed with some unreacted 9. Following this was the reduction of residual aldehyde functionalities using LiAlH$_4$ followed by acidification with 0.5M HCl solution. The mixture of compounds was extracted with ether and dried with anhydrous MgSO$_4$ to yield a mixture of 10 and 12.

9   10   11
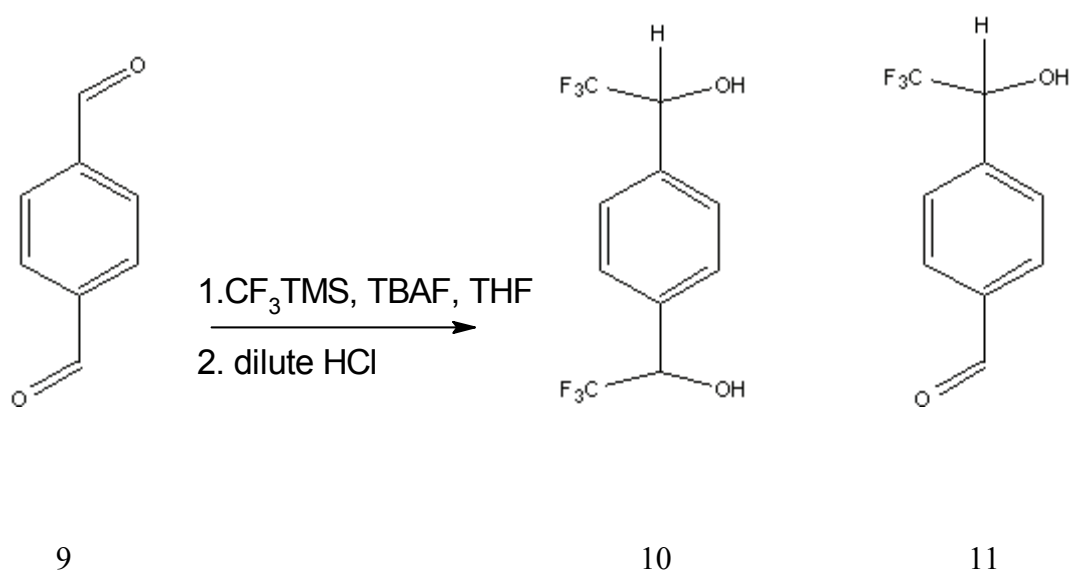
Scheme 3: Nucleophilic Trifluoromethylation
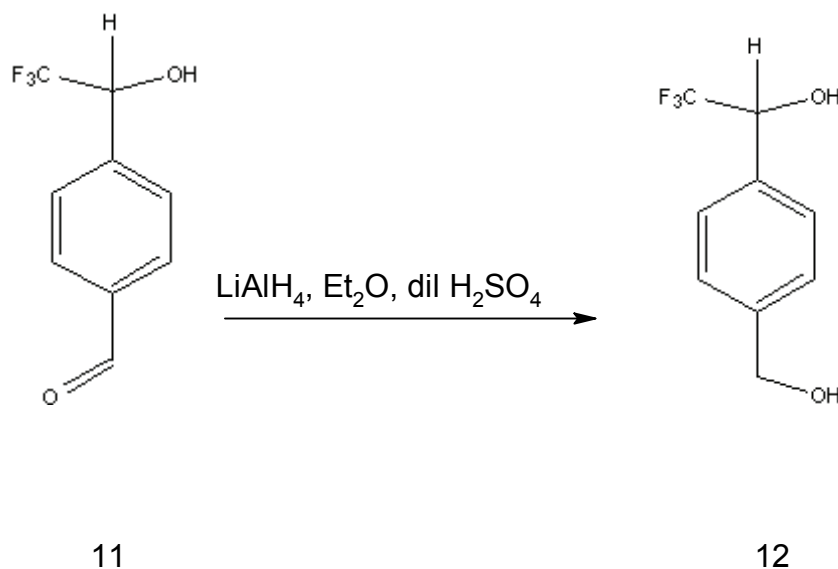
Scheme 4: Reduction of aldehyde functionality

The respective mono and bis-CF$_3$ diols were purified and separated via column chromatography using a 1:1 mixture of Ethyl Acetate/Chloroform. The bis-CF$_3$ diol eluted faster (R$_f$= 0.86) than the mono-CF$_3$ diol (R$_f$= 0.46) due to the presence of the trifluoromethyl groups and their electron withdrawing effect. The hydroxyl groups are Lewis basic and are attracted to the polar Lewis acidic silica gel of the column. The electron withdrawing effect of the trifluoromethyl group causes the basicity of the hydroxyl groups to decrease and therefore is less attracted to the polar silica gel and spends less time on the column. The diols were converted to various other functional groups which behave as leaving groups or polarizer in the subsequent polymerizations. Upon introducing various other functionalities, the chemical reactivity of the monomers changes by affecting their solubility in organic solvents, polarizability, leaving group ability, and thermal elimination to produce the pre-cursor polymer. The synthesis of these

other monomers, some interesting chemistry, and analytical data will be discussed in the following chapters.

Bis and Mono-CF$_3$ di Chloride Synthesis

The conversion of an alcohol to chloride is typically provided by the use of thionyl chloride, SOCl$_2$. The mixture of diols was dissolved in a solution of pyridine under nitrogen atmosphere. Thionyl chloride was added via syringe and the reaction was brought to reflux for a period of 24hr. The excess pyridine and thionyl chloride were removed via distillation; an equal amount of silica gel was added to the brown sludge and upon column chromatography produced the corresponding bis and mono-CF$_3$ chlorides (R_f = 0.46 and 0.45), respectively.
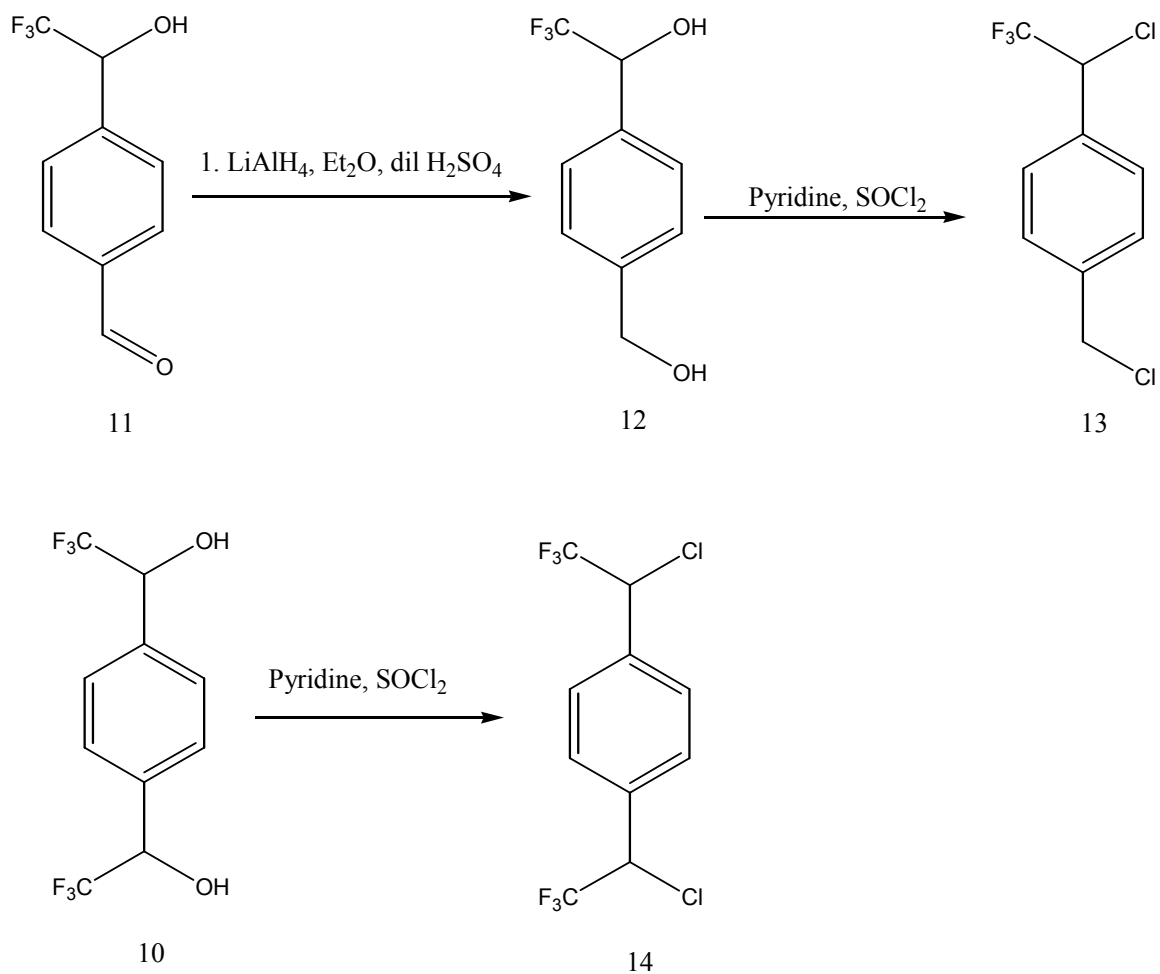
Scheme 5: Chlorination Reaction

Chapter 3: Other Synthesized Monomers

Introduction

The subsequent monomers produced were through various substitution reactions from the mono and bis-CF$_3$ dichloride or diol derivatives. There was interesting chemistry due to the presence of the CF$_3$ which controlled regioselectivity and unwarranted products were produced which we later exploited. There was also interesting chemistry in regards to the diols, again, also due to the presence of the trifluoromethyl group and its effect on the basicity of the hydroxyl group.

O- Ethyl Xanthate Monomers

The production of xanthates is provided by using a salt of the xanthic acid in this case Potassium *O*-ethyl xanthic acid, salt was used. A mixture of the dichlorides was dissolved in a solution of methanol along with the xanthic acid salt and left to stir overnight. A solution of saturated NaCl was then added along with dichloromethane and left to stir for 20 minutes. The product was extracted with dichloromethane, dried with MgSO$_4$, and purified via column chromatography to yield the mono CF$_3$ chloride xanthate (R$_f$=0.39). The reaction only occurred with the mono CF$_3$ di chloride derivative and substitution only occurred at the benzylic position not containing the trifluoromethyl group. The reaction with the bis CF$_3$ dichloride only gave back starting material and we were unsuccessful at converting the dichloride and the remaining chlorine in the mono CF$_3$ dichloride to their respective xanthate. Forced conditions such as longer reaction time, higher temperatures, higher concentrations of starting material, and the use of

different solvents did not provide the desired product.
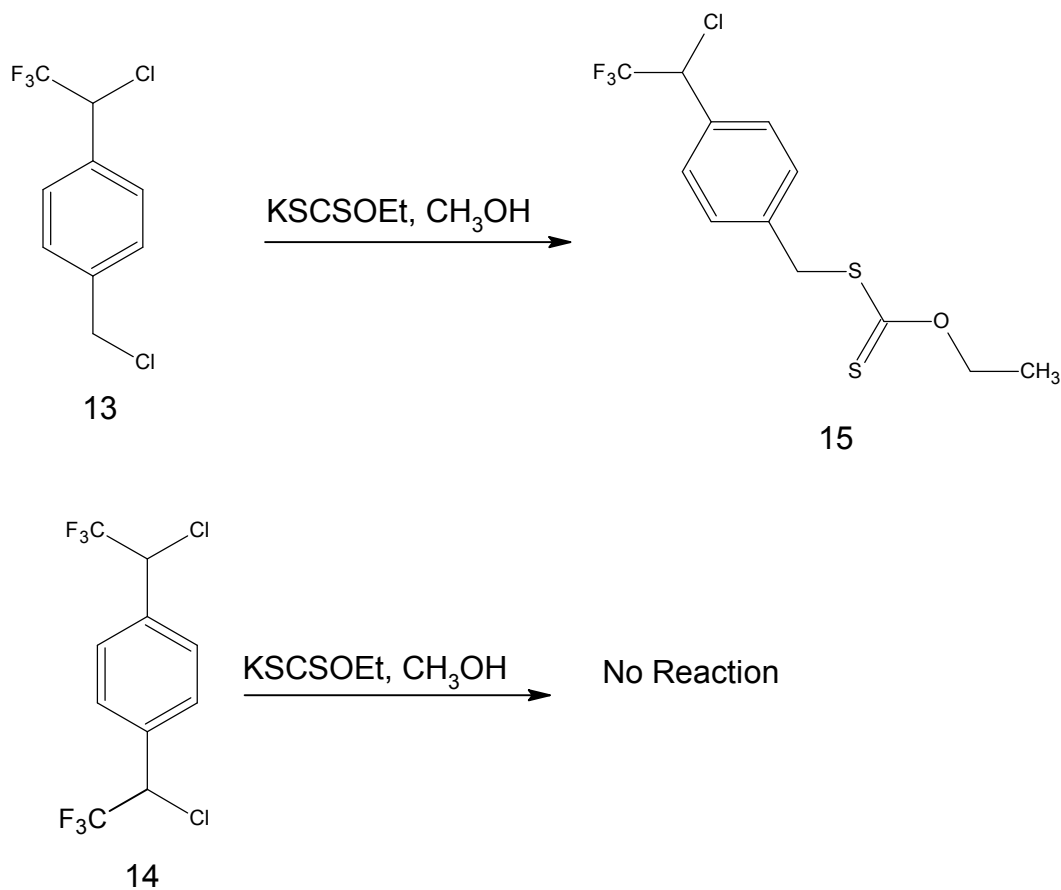
Scheme 6: *O*-Ethyl Xanthate Substitution

The reasoning behind this particular reaction and the observed formation of products is the presence of the CF_3 group. Studies have shown that the CF_3 retards the solvolysis of benzylic tosylates.[37] The electron withdrawing nature of the CF_3 group has been studied in structural motifs shown below for substitution reactions.

X = H

= OH
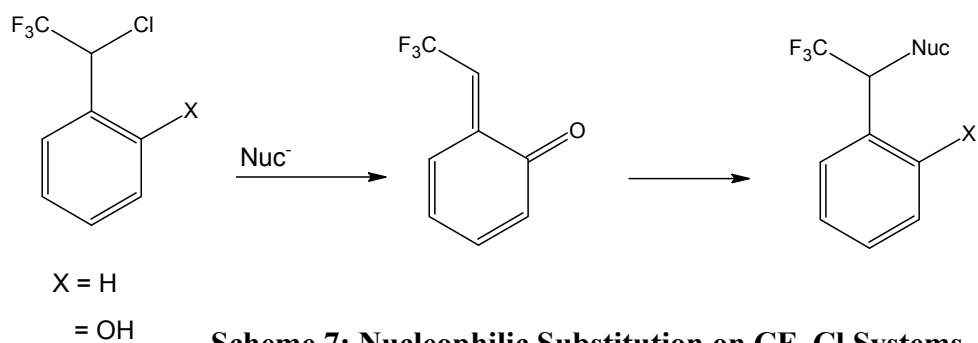
Scheme 7: Nucleophilic Substitution on CF_3 Cl Systems

The structure provides a mechanistic explanation for our reaction due to similar structural motifs. When X is a hydrogen atom there is no observed substitution, but when X is a hydroxyl group or an electron donating group a quinine methide intermediate can be formed. In the case where X is a hydrogen atom, the chlorine atom will be expelled on its own leaving behind a carbocation which is destabilized by the CF_3 group and explains why there is no substitution observed. If a hydroxyl group is present, the oxygen atom lone pairs are donated to form a resonance stabilized cation which is delocalized over the carbon that was bonded to the chlorine atom and the oxygen atom. The incoming nucleophile will attack the carbon-carbon double bond formed to give the product.[38]

S- Methyl Xanthate Monomer Synthesis

The introduction of the *O*-ethyl xanthate was unsuccessful, but the *S*-methyl xanthate could be introduced via the oxygen atom in the diol derivatives. A solution of sodium hydride in anhydrous THF was added under nitrogen atmosphere at room temperature. A solution of either diol in THF was added drop wise and left to stir for an hour, and then carbon disulfide was added. The solution was left to stir for another hour and then methyl iodide was added via syringe and left to stir overnight. An ice/water mixture was added to neutralize any excess sodium hydride followed by ether extraction. The product was purified through column chromatography giving the mono CF_3 xanthate alcohol or the bis CF_3 dixanthate (R_f= 0.40 9:1 hexane/ether and R_f=0.50 1:1 hexane/ether), respectively. In the mechanism, the sodium hydride deprotonates the hydroxyl group to give a stabilized anion through the electron with drawing effects of the trifluoromethyl group. The anion attacks the nucleophilic center of the carbon disulfide

expelling electron density onto the sulfur to yield a sulfide ion intermediate. This
intermediate does a nucleophilic attack via S$_N$2 on the methyl iodide to give the final
product. The reaction proceeds all the way until both hydroxyl groups have undergone
addition of the xanthate group.
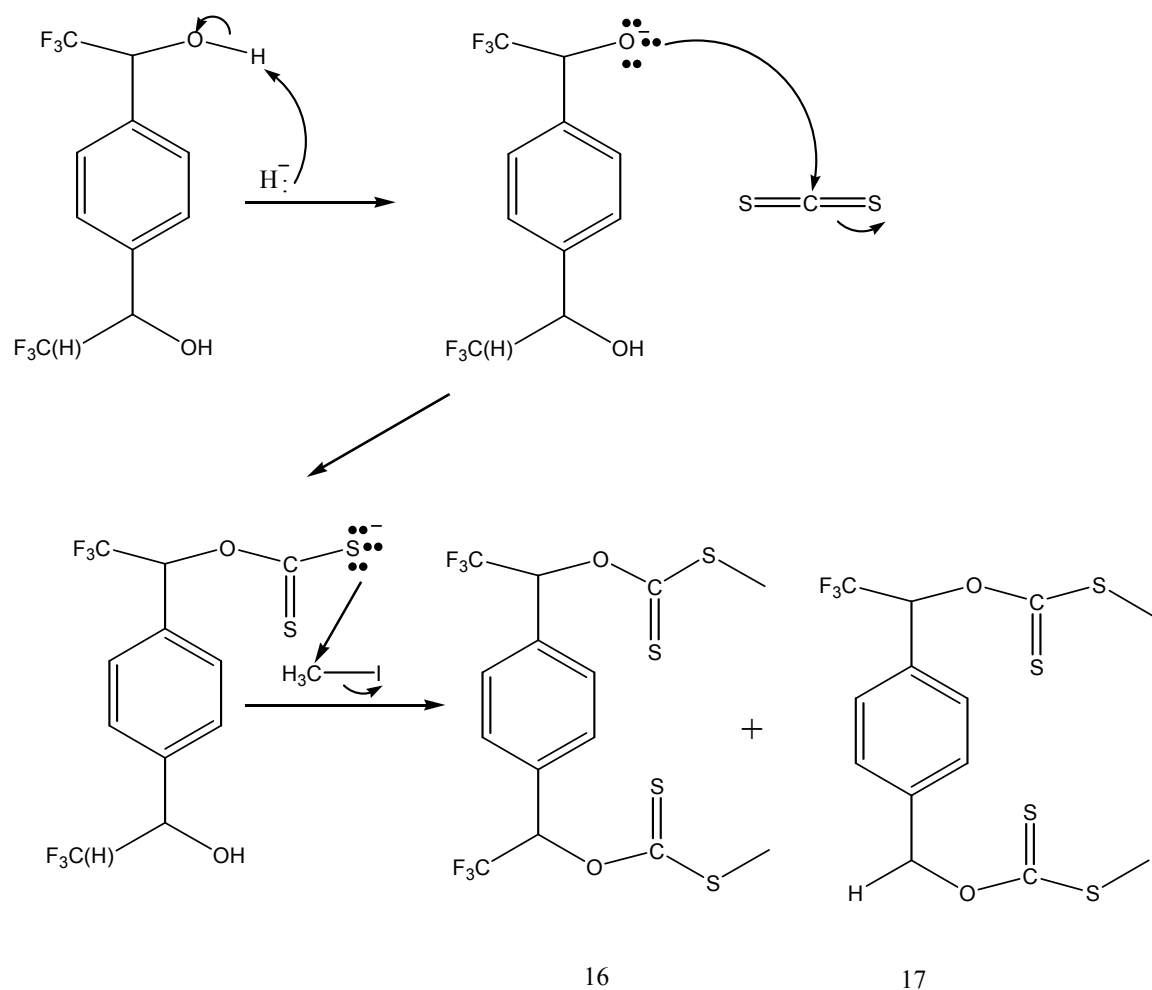
Scheme 8: *S*-Methyl Substitution Mechanism

Sulfinyl and Sulfonyl Monomer Synthesis

The sulfinyl and sulfonyl synthesis was carried out starting out from the mono
CF$_3$ chloride. A solution of n-Octane thiol and sodium t-butoxide in methanol was stirred
for half an hour at room temperature followed by the addition of a solution of the mono

CF$_3$ chloride in methanol. After an hour at room temperature, tellurium dioxide and

hydrogen peroxide were added and left to stir for another hour. A solution of saturated

sodium chloride and dichloromethane was added and left to stir. After an hour, an

extraction with dichloromethane, drying with anhydrous MgSO$_4$ and column

chromatography yielded the mono CF$_3$ chloro sulfoxide monomer. The sulfone monomer

was produced by the oxidation of the sulfoxide through the use of meta-

chloroperoxybenzoic acid (MCPBA). A solution of the sulfoxide monomer was cooled to

0° under nitrogen atmosphere, and over the period of 15 minutes a solution of MCPBA in

dichloromethane was added and left to stir for an hour at room temperature. After an

hour, a solution of sodium hydroxide and dichloromethane was added. Upon extraction

with dichloromethane extraction, drying with MgSO$_4$, and column chromatography

yielded our mono CF$_3$ chloro sulfone monomer.
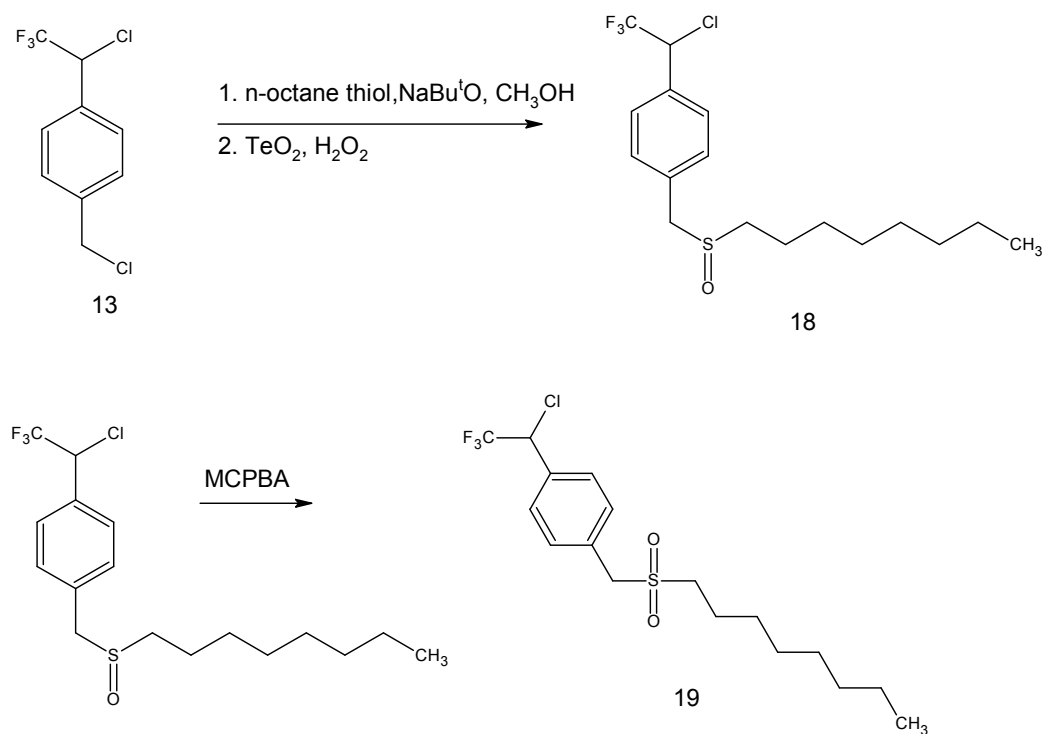
Scheme 9: Octane thiol substitution and oxidation

Substitution was only available at the non-CF_3 terminus despite forced reaction conditions such as increase in temperature, increased starting material concentrations, and longer reaction times.

Tosylate Monomer Synthesis and Reactions

The synthesis for introducing other functionalities from the chloro derivative monomers proved unyielding due to reasons discussed previously. The synthesis of incorporating the tosylate functionality (Tos) would hopefully provide a much superior leaving group than the chlorine atom, and the tosylate's superiority as a leaving group would more than compensate for the lack of stability in the carbocation formed. The introduction of a tosylate group is produced via the combination of *p*-toluenesulfonyl chloride (TosCl) and an alcohol to form a sulfonate ester. A solution of sodium hydride under nitrogen atmosphere in THF at room temperature, and a solution of the monomer was added drop wise to the stirred solution. After 50 minutes, a solution of TosCl in THF was added drop wise and the resulting yellow mixture was left to reflux overnight. After cooling to room temperature, ice added and an ether extraction was performed to yield the products.
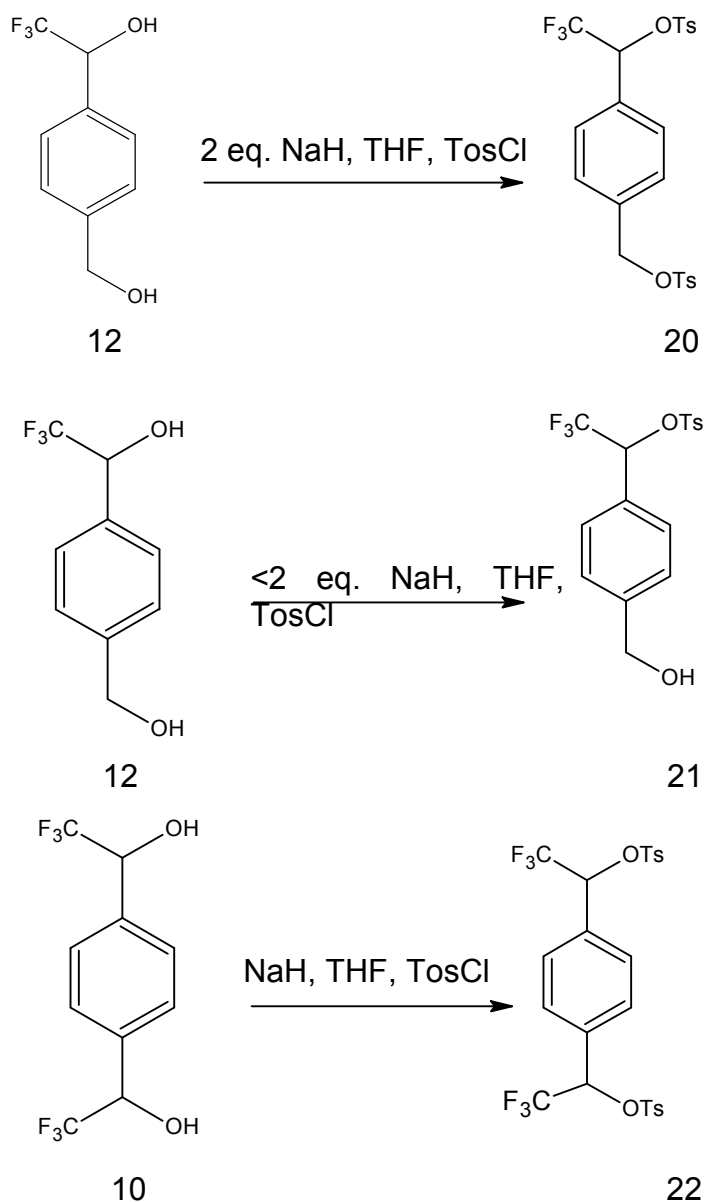
Scheme 10: Tosylate Synthesis

    The tosylate synthesis was successful and obtained two different products from the mono CF_3 diol monomer depending on the amount of base used. The use of 2 equivalents of base provides the conversion of both alcohol functionalities to the tosylate functionality. The use of less than 2 equivalents provides a single alcohol converted to the tosylate group, specifically, the alcohol bearing the CF_3 group. The CF_3 group

increases the hydroxyl group's acidity due to the stabilizing feature the CF_3 group provides the oxyanion formed through its electron withdrawing effects. Therefore it is this hydroxyl and not the other hydroxyl which will react to give the product. The synthesis of the tosylate monomers provided us with a way to incorporate other functionalities but not in the way we expected. The tosylate monomers were converted to the respective xanthate, sulfoxide, and sulfone. Unfortunately, forcing reaction conditions did not yield with substitution at both ends of our systems and only the non-CF_3 terminus reacted while the CF_3 terminus remained unaffected.

Tosylate Reactions

The mono CF_3 OTosylate was reacted further in order to make unsymmetrical monomers with varying substituents. As with the mono CF_3 chloro monomer, the CF_3 OTos monomer also showed substitution only at the non-CF_3 terminus. The OTosylate monomer was converted to the respective O-Ethyl Xanthate, Sulfoxide, and Sulfone as shown in Scheme 11:
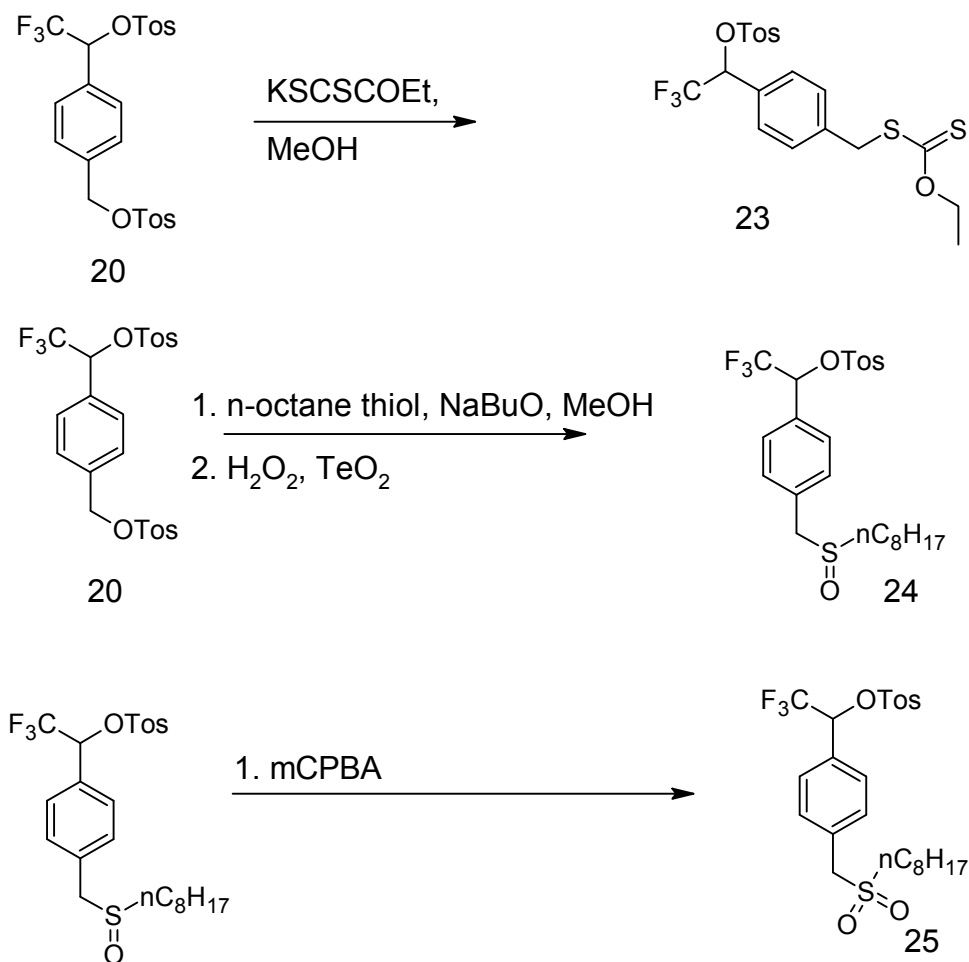
Scheme 11: Mono CF₃ OTos Substitutions

Triflate Monomer Synthesis

The triflate (OTf) is an excellent leaving group in substitution reactions; the synthesis of the triflate derivatives produced unexpected results. A solution of either the mono or bis CF$_3$ diols was dissolved in pyridine and cooled to 0°C. After stirring for an hour at this temperature, triflic anhydride was added via syringe turning the solution bright red. The solution was allowed to warm up to room temperature and left to stir for 4 hours. Ice was then added to the solution and brought to neutral pH and the aqueous layer was extracted with ether. ^{19}F NMR on the ether extraction showed no presence of fluorine but the aqueous layer did, and further characterization indicated the proposed

structures. It is concluded that the triflic anhydride substitution occurs followed by replacement by the solvent giving a pyridinium salt. An interesting observation in ^{19}F NMR of our product was the appearance of the fluoride ion NMR peak upon standing in aqueous base. It is proposed that the trifluoromethyl group is hydrolyzed to a carboxylic acid with the assistance of the proximate pyridinium group.
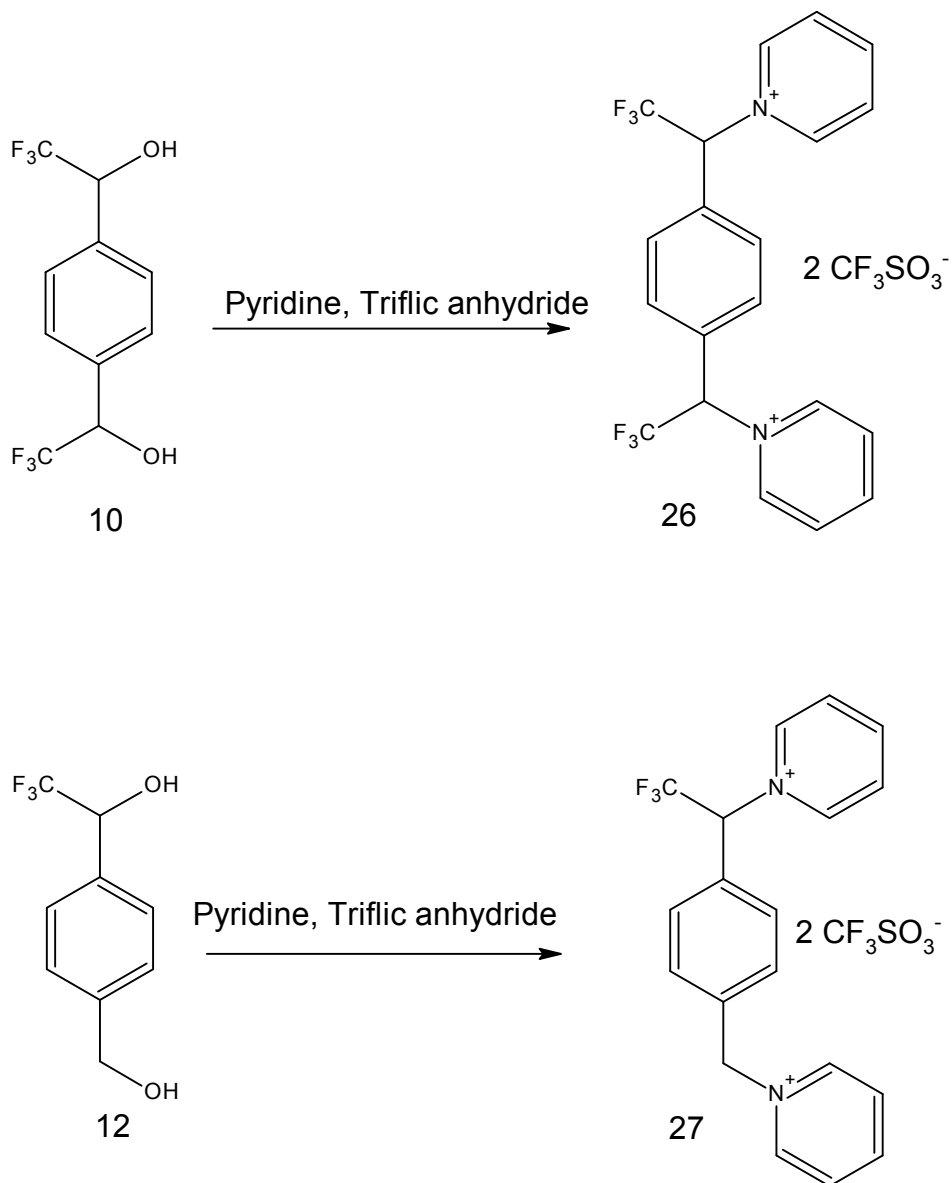
Scheme 12: Pyridine Synthesis

The ^{1}H NMR showed that the proton signal on the carbon bearing the CF_3 group changes from a quartet into a singlet. The ^{19}F NMR signal changed from the typical CF_3 signal into a fluoride ion signal indicating the loss of the trifluoromethyl group.

Chapter 4: Enantiomeric and Diastereomeric NMR

Stereochemistry is an important aspect of organic chemistry mainly in the area of

pharmaceutical chemistry, but stereochemistry is also important in polymer synthesis and

in determining the physical and electronic properties of the polymer produced.

Enantiomers are compounds that are non-super imposable mirror images of each other.

An asymmetric carbon atom consists of a carbon atom which has four different atoms, or

groups of atoms, bonded to the central carbon atom. The nomenclature of enantiomers is

given by the Cahn-Ingold-Prelog convention[39] in which priorities are assigned to each of

the four groups based upon their atomic number. An example shown below depicts the

nomenclature of a pair of enantiomers.
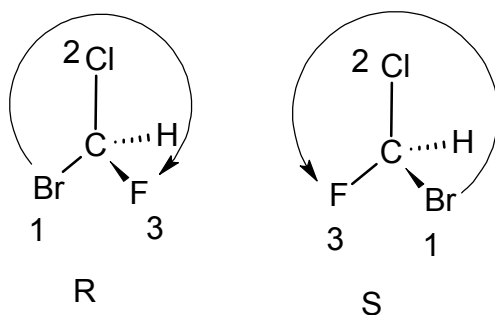
Enantiomers differ in many respects and one is the rotation of polarized light.

Enantiomers have the exact same physical properties (boiling point, melting point, etc).

The rotation of polarized light is an experimentally determined value and has no

correlation with the assignment of R or S nomenclature. Due to the complexity of some

organic compounds there can exist more than one stereo center of interest in the given

structure. One such case is one where stereoisomers which are not mirror images of one

another; such types of compounds are designated as diastereomers. Compounds which

have more than one stereoisomer but have a mirror plane of symmetry are deemed to be

meso compounds. When analyzing a compound with *n* number of stereocenters, the 2^n

rule will give the maximum number of stereocenters the given compound may have. Such

an example is given below for 2,3-dibromobutane.

| (2R,3R) | (2S,3S) | (2R,3S) | (2S,3R) |
| 28 | 29 | 30 | 31 |
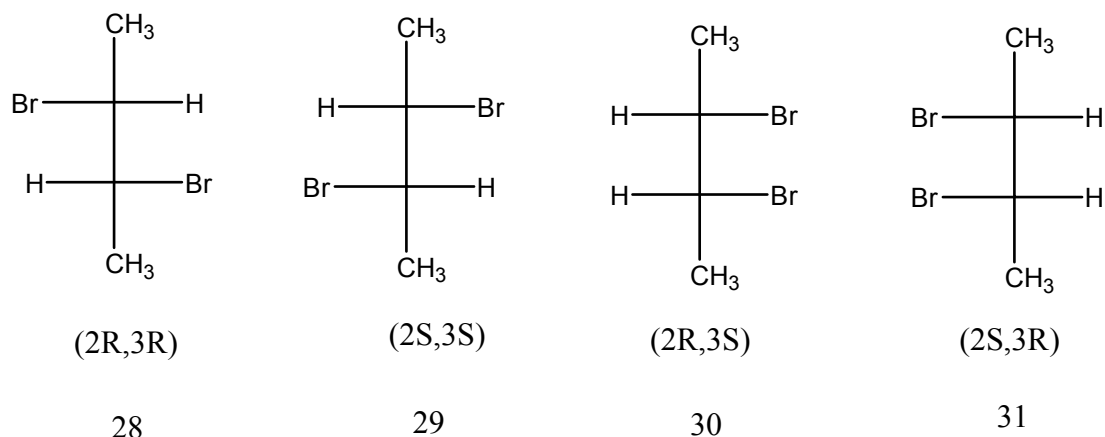
Figure 7: Diastereomers of 2,3 dibromobutane

Compounds 28 and 29 are enantiomers of another whilst 30 and 31 are meso

compounds due to the mirror plane of symmetry through the center of the molecule.

Compounds 28 and 29 are diastereomers of compounds 30 and 31. Compounds 28 and 29

are designated as the (*dl)* diastereomers while compounds 30 and 31 are designated as the

meso diastereomer. Unlike enantiomers, diastereomers do differ in their physical

properties; such an example is *trans*-2-butene with a boiling point of 0.9^oC and *cis*-2-

butene with a boiling point of 3.7^oC.

Diastereomers in NMR

The full multi dimensional NMR analyses of these monomers was reported by Dr.

Roche in the Magnetic Resonance in Chemistry journal.[40] Due to the asymmetric nature

of most of the compounds containing the same or different functionalities on both

benzylic positions our NMR proved to be very interesting. One such example is the mono

CF$_3$ diol which has one stereo centric carbon atom and thus must come in enantiomeric pairs.
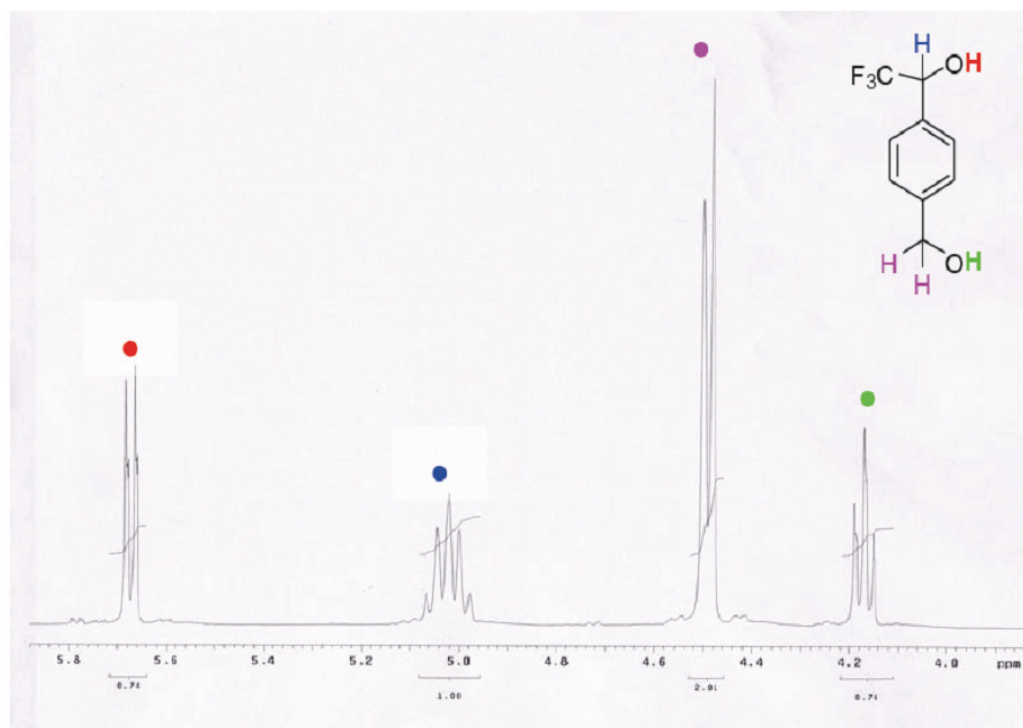
Figure 8: Proton NMR for Mono CF$_3$ diol

The ^{1}H NMR shown in Figure 8, is rather straight forward with only four of the NMR signals shown here. There are several interesting pieces of information that can be extracted from this spectrum. The presence of the trifluoromethyl group shows a dramatic downfield effect on its neighboring hydroxyl group's chemical shift from a typical 3-4ppm to 5.7ppm. The other hydroxyl group, highlighted in green, remains unaffected as a triplet due to the presence of its neighboring protons highlighted in purple. The benzylic proton bearing the trifluoromethyl group shows an interesting array of peaks. The benzylic proton couples with the three fluorine atoms and the hydroxyl proton (red) providing a multiplet. The benzylic proton's coupling constant with the trifluoromethyl group and the coupling constant with the hydroxyl group are close in value. The benzylic

proton can be thought of as either a doublet of quartets or a quartet of doublets which overlap to give the apparent pentet. All of the structural motifs bearing only one trifluoromethyl group resembled the same type of NMR spectrum with minor chemical differences.

Other compounds which bear a single trifluoromethyl group and varying substituents on the benzylic carbon or the bis CF_3 di substituted monomers also provided interesting NMR data. These systems are diastereoisomers due to the presence of two stereocenter carbon atoms and give rise to a meso and (*dl*) diastereomers. One such case was the bis CF_3 di Tos monomer which produced the following spectrum:
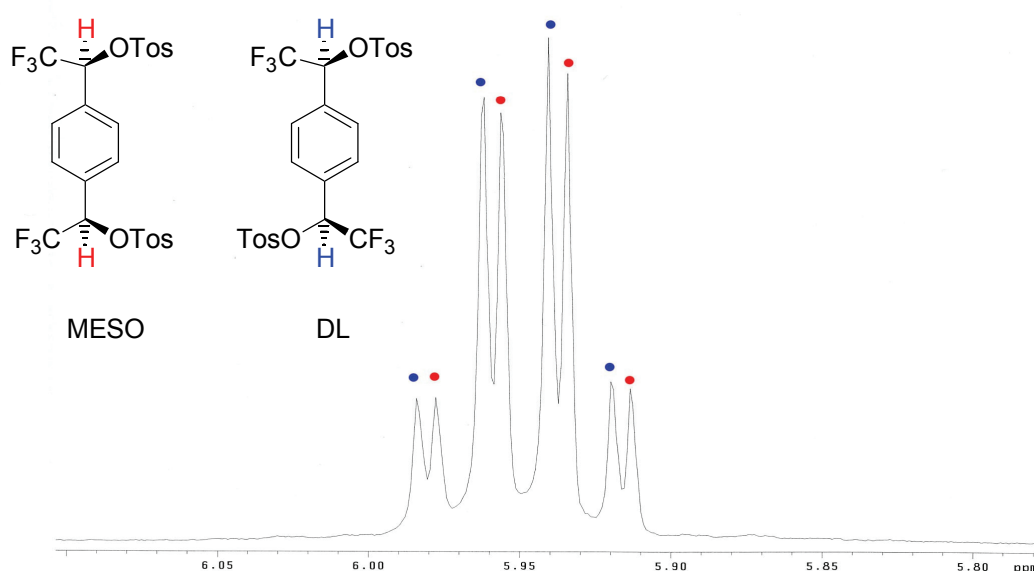
Figure 9: Bis CF$_3$ di OTos ^{1}H NMR Spectrum

The spectrum in Figure 9 only focuses on the benzylic proton signals mainly to focus on the diastereotopic hydrogens. The spectrum appears to show four sets of doublets upon first inspection, but in reality these seemingly four doublets are two quartets superimposed upon one another. The benzylic proton is called a diastereotopic

hydrogen due to it being bound to a carbon atom which exhibits diastereometric stereochemistry. Each diastereomer, the meso and dl, give rise to their own quartet caused by the splitting of the three neighboring fluorines and the spectrum above is obtained.

The ^{13}C NMR showed very similar peak patterns for the systems. One such example is the bis CF_3 S-methyl xanthate monomer and its spectrum shown below:
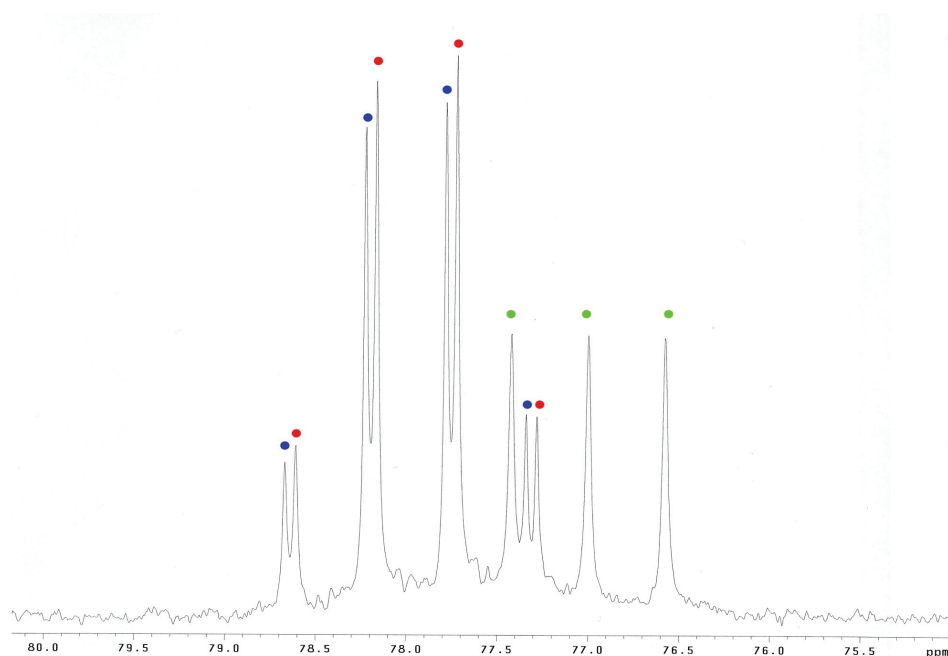
Figure 10: S-Methyl Xanthate ^{13}C NMR

The ^{13}C NMR spectrum shown above has the exact same pattern of peaks as did the ^{1}H NMR for the other system. At first inspection one suspects to see four doublets in

the spectrum but with further inspection it is determined that they are actually two overlapping quartets due to the splitting by the three neighboring fluorine atoms. In ^{13}C NMR, the carbon and hydrogen atoms are decoupled in order to avoid complex splitting but not the carbon and fluorine atoms and will thus give rise to splitting. The $2NI + 1$ rule is used to find the splitting between any two neighboring atoms where N is the number of neighboring atoms and I is the spin of the nucleus of the neighboring nuclei under observation. The triplet peak highlighted in green is due to the deuturated chloroform solvent, $CDCl_3$, used for NMR sampling. The spin of the nucleus under observation is typically I=1/2 so the $2NI + 1$ rule reduces to N + 1, but this is not the case with deuterium in which its spin is I=1. The carbon and deuterium are not decoupled therefore the splitting given by the $2NI + 1$ rule is the triplet observed in the spectrum.

Another system which gave interesting NMR data was our mono CF_3 OTosylate Sulfoxide monomer shown below:
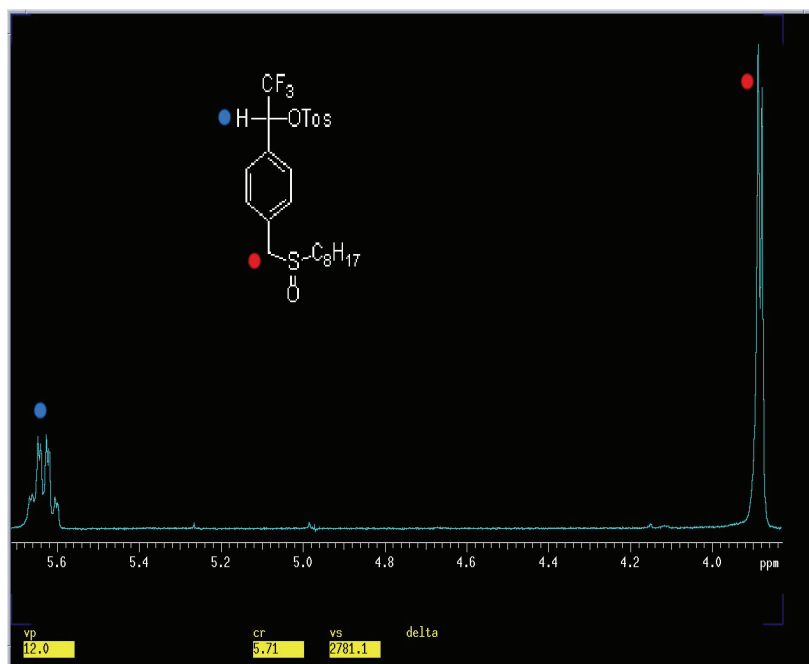
Figure 11: Mono CF$_3$ OTos Sulfoxide ^{1}H NMR

Upon initial inspection of the structure one would suspect to find a quartet by the benzylic hydrogen bearing the CF_3 group and a singlet from the other benzylic hydrogens. This is not the case, in fact, as with each diastereomeric hydrogen or carbon atom, each diastereomer will give rise to their individual NMR signal. The benzylic hydrogen highlighted in blue is an overlap of two quartets which looks complex without further zooming in on the spectrum. The hydrogen atom highlighted in red gives rise to two singlets which on initial inspection look like one doublet. The sulfoxide group exists as a tetrahedral arrangement in which it places its lone pairs in an sp^3 orbital making the protons on the benzylic carbon diastereomeric and thus each diastereomer gives rise to their signal.

Chapter 5: Theoretical NMR Studies

Introduction

Due to the fact that it is impossible to experimentally identify a pair of

enantiomers using conventional NMR techniques, we used Gaussian[41] to determine

whether or not we could theoretically identify a set of diastereomers. The specific

molecule under study was the bis CF_3 di S-Methyl Xanthate.

meso diastereomer (S,R)   (*dl*) diastereomer (S, S)
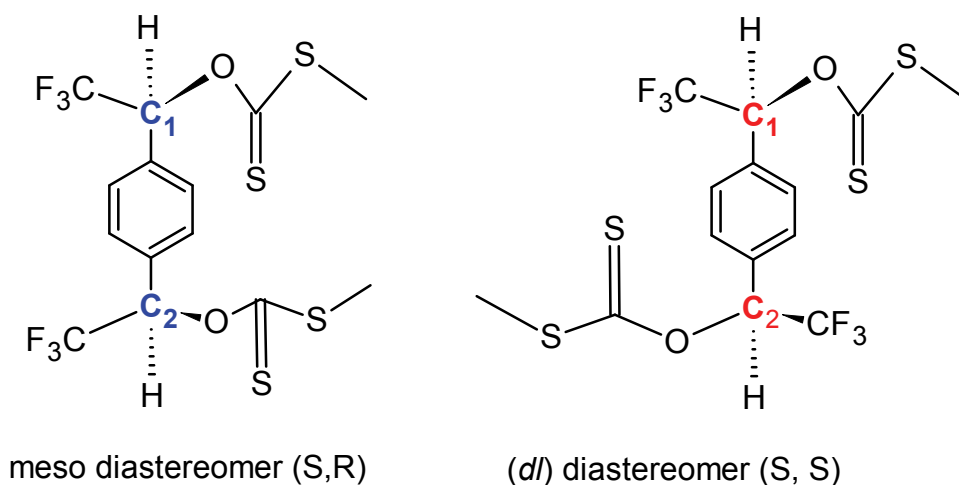
Figure 12: S-Methyl Xanthate Diastereomers

The bis CF_3 di S-Methyl Xanthate system contains two carbon stereocenters as indicated

by the blue and red carbon atoms as shown in Figure 12. The symmetrical system is

designated as the meso compound while the unsymmetrical compound is designated as

the (*dl*) compound. Seven initial guesses to the meso geometry were obtained by rotating

the two substituted xanthate groups, and seven geometry optimizations yielded two

unique structures. A totally eclipsed geometry(1) where the trifluorormethyl groups are

perpendicular to the plane of the benzene ring, or the anti geometry(2) where the dihedral

angle between the two trifluorormethyl groups is 180°. The geometries for the seven

different geometries for each diastereomer were optimized and their energies calculated

using a 6-31g(d) basis set and the theoretical NMR shifts using 6-311+g(2d,p) basis set. In addition a B3LYP density functional was used for all calculations. [42, 43] The two geometries of lowest energy are:

 Eclipsed meso   E = -2882.96735805   A.U. = -1809602.017176375 kcal/mol

anti meso   E = -2882.96755312   A.U. = -1809602.1395828 kcal/mol

The difference in energy between the two geometries is 0.122651625 kcal/mol and is negligible as is for the eclipsed and gauche *dl* geometries. From the two molecules of lowest energy for each diastereomer we calculated the theoretical ^1H, ^{19}F, and ^{13}C NMR shifts in deuterated chloroform ($CDCl_3$) as a solvent and TMS(trimethylsilane) and $CFCl_3$(trichlorofluoromethane) as the standard references, respectively.

Meso NMR Discussion

The following images are for the optimized geometries of the meso compound:
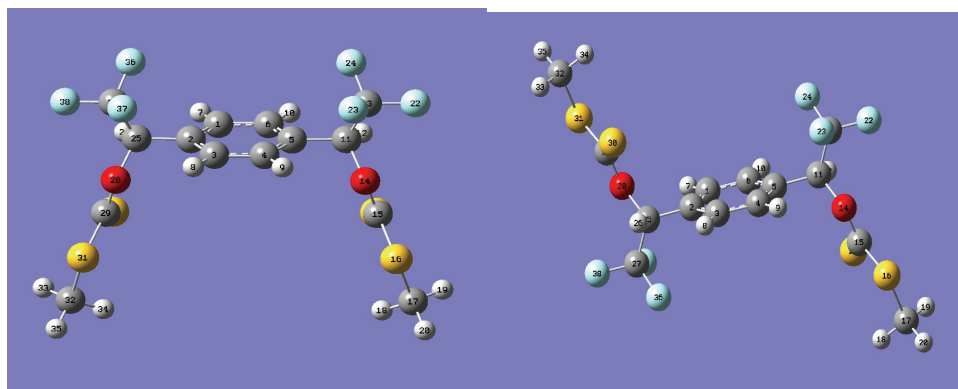
Eclipsed meso   Anti meso

Figure 13: Optimized Geometries for meso S-Methyl Xanthate

biscf3 di O xan

Pulse Sequence: s2pul

Solvent: CDCl3
Ambient temperature
File: biscf3diOxan-19F
Mercury-300BB "chemnmr01.rutgers.edu"

Relax. delay 4.000 sec
Pulse 32.1 degrees
Acq. time 0.300 sec
Width 80000.0 Hz
16 repetitions
OBSERVE F19, 282.2441957 MHz
DATA PROCESSING
Line broadening 0.3 Hz
FT size 65536
Total time 2 min, 24 sec

-74.920 -74.946

-74.0   -74.2   -74.4   -74.6   -74.8   -75.0   -75.2   -75.4   -75.6   -75.8   -76.0   -76.2   -76.4   ppm

Figure 14: ^{19}F NMR of S-Methyl Xanthate

Eclipsed Meso F #s	Theoretical NMR Shifts (ppm)	Average Value(ppm)	Overall Value(ppm)
22	-79.3479	-80.7563	-80.999
23	-86.8348		
24	-76.0863		
36	-76.0863		
37	-86.8348		
38	-79.3479		
Anti meso F #s			
22	-79.7103	-81.2418	
23	-86.7691		
24	-77.2461		
36	-77.2442		
37	-86.7696		

38	-79.7105		
Eclipsed *dl* F #s			
14	-79.9904	-81.503	-81.901
15	-77.4592		
16	-87.0596		
28	-87.0596		
29	-79.9904		
30	-77.4592		
Gauche *dl7* F #s			
14	-80.0987	-82.2996	
15	-77.3273		
16	-89.4728		
28	-89.4780	-82.2990	
29	-80.0960		
30	-77.3230		

Table 5: Meso and *dl* Theoretical ^{19}F NMR shifts

In theory there should be three different chemical shifts for the fluorine atoms
based on the electron's interaction with a magnetic field and the interaction of the nuclear
magnetic moments with a magnetic field. The theoretical shifts are calculated from the
second derivative of molecular energy with respect to the magnetic field and the nuclear
magnetic moments. The method used is the Gauge Invariant Atomic Orbital (GIAO)
method. For the eclipsed and anti meso compounds, the fluorine NMR shifts of atoms 22,
23, and 24 correspond with atoms 36, 37, and 38 due to the symmetrical nature of both
geometries. The same scenario holds true for the fluorine NMR shifts of the dl
geometries; the overall value for the trifluorormethyl shift for the *dl* geometry is -81.901
ppm. There is a very small difference of about 2 ppm between the meso and *dl* fluorine
NMR shift which is indicative that you may be able to experimentally identify each
diastereomer.

Gauche dl   *eclipsed dl*
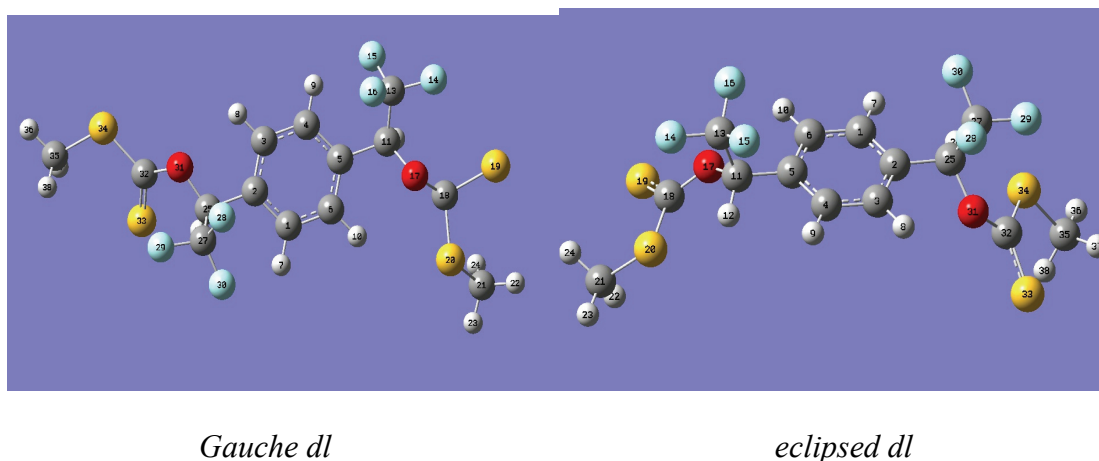
Figure 15: Optimized Geometries for *(dl)* S-Methyl Xanthate

Type of H	Eclipsed meso	Anti meso	*Gauche dl*	*Eclipsed dl*
Aromatic	7.8749	7.8673	8.6770[*]	7.8288
Benzylic	7.0324	7.0138	7.9986[*]	6.9812
Methyl	2.479	2.5294	2.7230[*]	2.505

Table 6: Summarized ^{1}H Theoretical NMR Shifts (*represents average shift values)

As seen from this summarized table of theoretical NMR shifts for the protons in the diastereomers, the eclipsed meso and anti meso compounds have fairly similar chemical shifts. This isn't surprising since both structures have similar energies and will thus produce similar NMR spectra. The ^{1}H NMR shifts of the eclipsed *dl* geometry and gauche *dl* geometry are only similar for the methyl protons, but not the aromatic or benzlyic protons due to differences in dihedral angles. The experimental values for the NMR shifts of our bis CF$_3$ di S-methyl xanthate system are as follows: ^{19}F NMR (-74.93 ppm) and ^{1}H (7.53, 6.96, and 2.62 ppm). The orders of the hydrogen shifts are for the aromatic, benzylic, and methyl hydrogens, respectively. Table 7 below summarizes the ^{13}C theoretical NMR shifts for the meso compounds.

43

Meso C #s	Eclipsed Meso Theoretical NMR Shifts(ppm)	Anti Meso Theoretical NMR Shifts(ppm)
Stereocenter C		
11	83.8059	83.8308
25	83.8059	83.8304
CF$_3$ C		
13	134.1465	134.0689
27	134.1465	134.0689
Xanthate C		
29	231.3645	231.3443
15	231.3645	231.3448
Methyl C		
32	25.6769	25.9235
17	25.6769	25.9234
Aromatic C		
1	136.8916	134.1548
2	139.6613	140.706
3	134.9089	137.363
4	134.9089	134.1548
5	139.6613	140.7067
6	136.8916	137.3627

Table 7: ^{13}C NMR Meso Theoretical NMR Shifts

As seen from Table 7, the same pattern occurs for the theoretical ^{13}C NMR shifts as did for the ^{1}H and ^{19}F NMR shifts. The theoretical values remain unchanged and are also the same for each type of carbon atom due to the symmetry of the eclipsed and anti meso compounds. Table 8 below summarizes the ^{13}C theoretical NMR shifts for the *dl* geometries.

dl C #s	Eclipsed *dl* Theoretical NMR Shifts(ppm)	Gauche *dl* Theoretical NMR Shifts(ppm)
Stereocenter C		
11	83.6438	85.0023
25	83.6438	85.004
CF$_3$ C		
13	134.0859	133.3489
27	134.0859	133.3496
Xanthate C		
18	231.4559	223.7696
32	231.4559	223.7692
Methyl C		
21	25.8286	27.3789
35	25.8286	27.3784
Aromatic C		
1	137.0319	134.6467
2	140.5094	139.8705
3	134.0180	134.0608
4	137.0319	134.6435
5	140.5094	139.8715
6	134.0180	134.0592

Table 8: *dl* ^{13}C Theoretical NMR Shifts

In summary, the ^{13}C NMR shifts are very similar for both dl geometries, but there is a small difference in chemical shifts. The stereocenter carbon atom for the meso compound is 83.8183 ppm and that for the *dl* geometry is 84.430 ppm. The largest difference of 7 ppm is for the xanthate carbon atoms for the eclipsed and gauche dl geometries with values of 231.4559 and 223.7696, respectively. As with the case for the fluorine NMR shifts, there is a small difference in NMR shift values, but the ^{13}C NMR values again show a small indication that the diastereomers may be differentiated experimentally.

Chapter 6: Mass Spectrometry

All the monomers were also characterized via high resolution mass spectrometry along with ^{1}H, ^{19}F, and ^{13}C NMR. Mass Spectrometry is useful to organic chemists because it provides the molecular weight. Mass Spectrometry measures the mass to charge (m/z) ratio of the fragments from your compound through various mechanisms. One such mechanism, electron impact, is used to bombard high speed electrons in order to eject an electron from the molecule. This process leaves behind a radical cation which can fragment to give radicals and cation fragments.

$$M + e^- \longrightarrow [M]^{+ \cdot} + 2e-$$
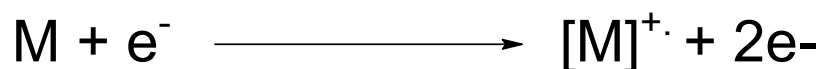
One such example is for the mono CF$_3$ di chloro system shown below:
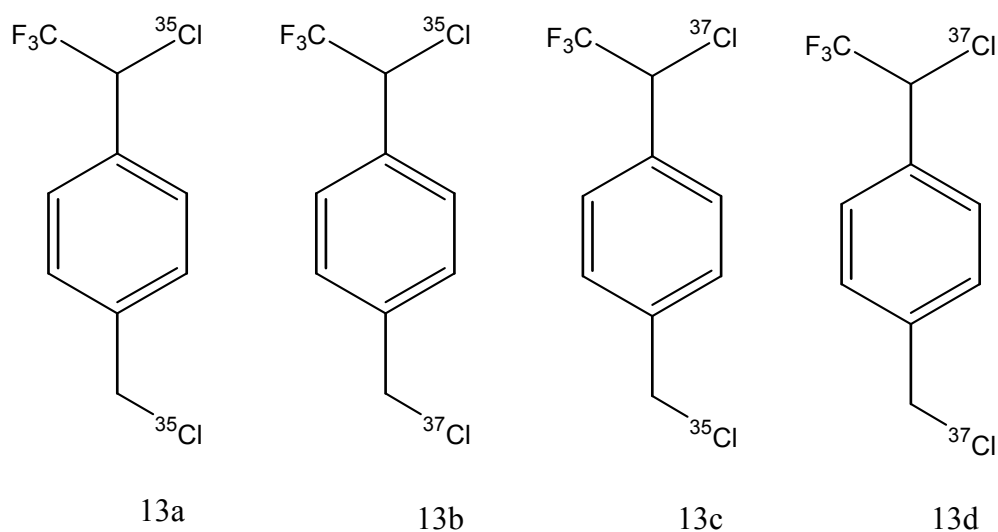
Figure 16: Mono CF$_3$ di Cl Isotopes

Masses	242	244	246
Chlorine Isotope Combination	13a	13b,13c	13d
Probability of Occurrence	1x (0.75)(0.75)	2x(0.75)(0.25)	1x(0.25)(0.25)
Percent Abundance	56.25	37.5	6.25

Table 9: Mono CF$_3$ di Cl Molecular Ion Percent Abundances

Initially, a high-speed electron will eject an electron from the chlorine atom leaving behind a radical cation. This radical cation will fragment in order to give radical and cationic species, but only the cationic species are detected by the mass spectrometer detector such as a quadropole or TOF(time-of-flight). Due to the presence of the chlorine atom, the true molecular weight is a combination or average of all the possibilities. The chlorine atom exists as two naturally occurring isotopes, namely ^{35}Cl and ^{37}Cl which contribute about 75 and 25 percent of chlorine's atomic weight, respectively. The probability of observing one molecular weight over another is determined by which isotope of chlorine is present in the molecule. The monomer consisting of two ^{35}Cl has the highest probability due to its highest natural abundance. The monomer consisting of one ^{35}Cl and one ^{37}Cl will be of lower probability due to the low abundance of ^{37}Cl. The monomer consisting of two ^{37}Cl will have the lowest of all probabilities of being

observed because of its low abundance. The mass spectrum for our given compound is shown below:
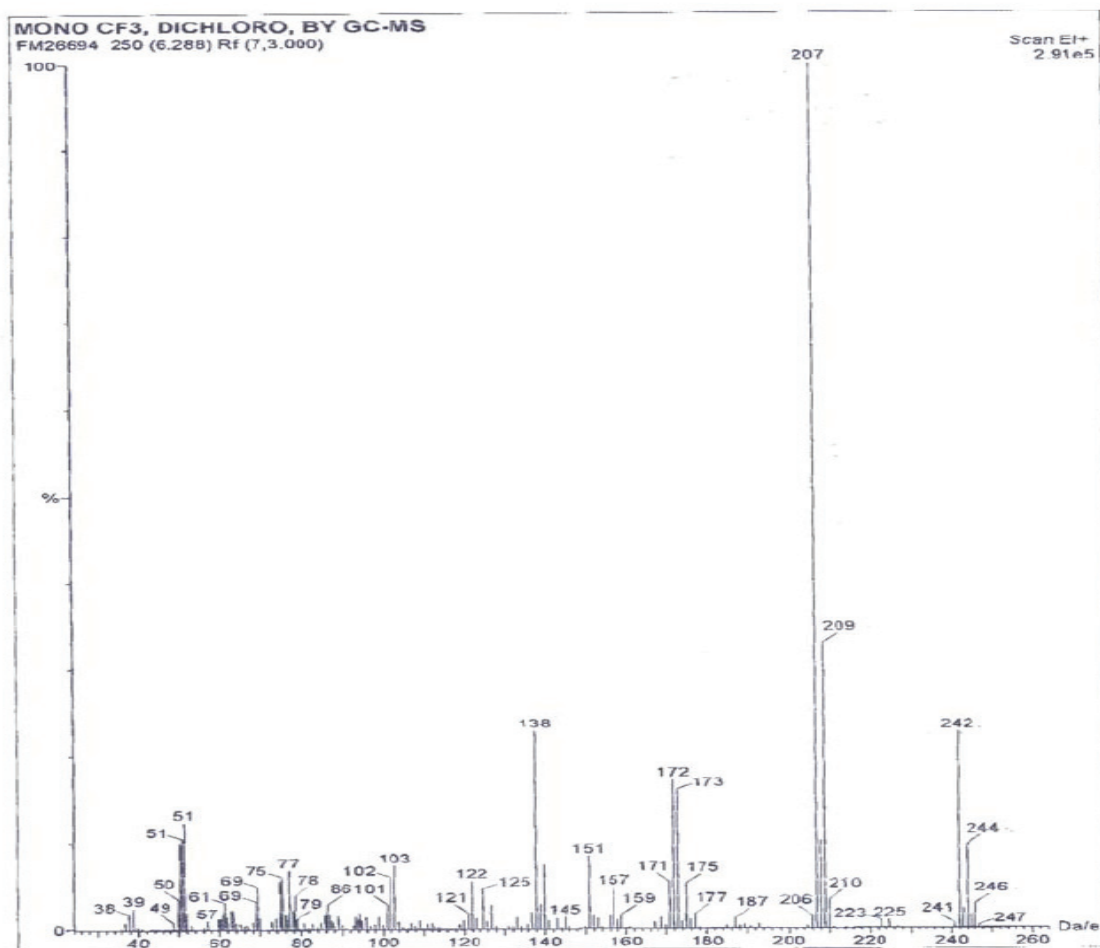
Figure 17: Mass Spectrum for Mono CF$_3$ di Cl

We see from this spectrum that the highest peak corresponds to the ion with molecular weight of 207. This corresponds to the loss of a chlorine atom (m=35) from compound 13a and the loss of a chlorine atom (m=37) from compounds 13b,13c shown in the table above. The chlorine atom which is removed is the chlorine atom which will leave behind the most stable species; the most stable species formed will be a carbocation on the benzylic carbon atom not bearing the CF$_3$ group. Due to the electron withdrawing nature

of the CF_3 group, a carbocation on the benzylic carbon bearing this group would be highly energetic and unstable. The other benzylic carbon atom would leave behind a primary carbocation which is resonance stabilized by the aromatic benzene ring. Next to the base peak we also observe the M+2 peak of 209 which is one third as large as the base peak and corresponds to the loss of a ^{35}Cl and ^{37}Cl from 13b,13c and 13d, respectively. On closer inspection to the right of the base peak we also see the peaks corresponding to compounds 13a, 13b, and 13c in much lower percentages due to their fragmentations to more stable species. To the left of the base peak we observe peaks corresponding to the loss of the CF_3 group at 173, 175, and 177, respectively from compounds 13a, 13b, and 13c. Another interesting peak further to the left corresponds to the loss of a CF_3 and a chlorine atom from compounds 13a and 13b giving a peak of 138. An important note to make for compound 13b is to keep track of which isotope is lost at the benzylic position. If a ^{37}Cl is lost, the peak will be 138, but if a ^{35}Cl is lost, the peak will be 140. The loss of a chlorine atom from compound 13c will also give rise to a peak of 140. The higher probabilities of 13a and 13b(^{35}Cl loss) occurring over 13b(^{37}Cl loss) and 13c gives rise to a higher peak. The last interesting peak is the peak at 103 which corresponds to the loss of a CF_3 and two chlorine atoms; interestingly this peak is due to the loss of a CF_3 and two chlorine atoms from compounds 13a, 13b, and 13c. Lastly the loss of a fluorine atom occurs and is observed at a very small peak of 223.

Chapter 7: Future Considerations:

The subsequent polymerizations were investigated by Anne D. Loyle, but insufficient material was used for proper polymerization, characterization, and isolation. An attempt in up-scaling from 5-10 grams of starting material into the 40-50 gram level of the diol monomer synthesis was made but it provided many isolation and purification problems. The use of high volumes of solvents, 500-1000mL for the reactions, purifications, and isolation also yielded complications. There were considerable amounts of trouble in separating our starting material, terephthaldicarboxaldehyde, from the products of the trifluoromethylation reaction. The reduction of our mixture of products from the trifluoromethylation reaction warranted even greater complications in isolation due to the complexity of the mixture of compounds and their affinities for the organic or aqueous layers. We moved on to the chlorination process but this also yielded frustrating result in isolation and purification. Returning to small-scale synthesis was no longer an option as we had already used all of our CF_3-TMS for the trifluoromethylation reaction. The process of isolating a single compound, our mono CF_3 diol from which all other subsequent monomers are produced, at considerably higher scales provides many problems which may be circumvented using other synthetic schemes. The production of the monomer via trifluoromethylation and reduction may not be the best route possible at larger scales. The following reaction has been proposed in order to synthesize the monomer and only the monomer and circumventing byproducts.
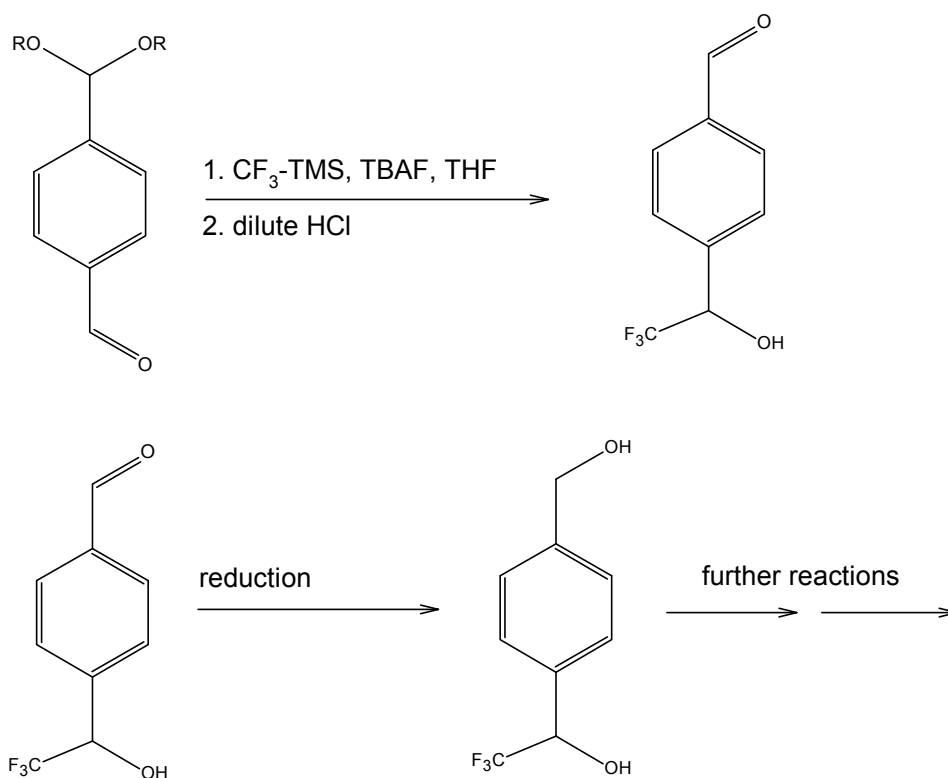
Scheme 13: Aldehyde Protection

The protection of aldehyde and ketone functionalities is widely used in order to achieve a specified product. Such is the case as shown in Scheme 13 in which the protection of only one aldehyde group, followed by trifluoromethylation and deprotection, and lastly the reduction in order to achieve the desired product. This process can be achieved by the use of ethylene glycol in a solution of a catalytic amount of TosOH in a solution of benzene. A problem which this procedure is the kinetic control of aldehyde protection and the production of byproducts. A way to circumvent this problem would be to begin with a system in which one aldehyde group is already protected but these compounds are highly expensive to purchase. The upscale process is currently underway in order to achieve sufficient amounts of products to further investigate the polymerization reactions.

Chapter 8: Experimental Section[28]

General Experimental Detail

All NMR spectra were obtained on a Varian Mercury Plus 300 MHz spectrometer with 5 mm ATB probe at ambient temperature. All ^{19}F, ^{1}H and ^{13}C NMR spectra were performed in $CDCl_3$ at 282, 300 and 75 MHz except where noted. Chemical shifts for ^{19}F, ^{1}H, and ^{13}C spectra were determined relative to $CFCl_3$ (0.00 ppm), residual $CHCl_3$ (7.24 ppm) and $CDCl_3$ (77.0 ppm), respectively. All products were white solids, except where specified. All reagents, unless otherwise specified, were used as purchased from Aldrich or Fisher. Column chromatography was performed using chromatographic silica gel 200-425 mesh, as supplied by Fisher. Melting points are uncorrected. Low-resolution mass spectrometry was performed at the Center for Advanced Food Technology, New Brunswick, NJ, and high-resolution mass spectrometry was performed at the University of Pennsylvania, Philadelphia, PA.

1-(1-Hydroxy-2,2,2-trifluoroethyl)-4-(hydroxymethyl)benzene (12) - 1,4-bis-(hydroxyl-2,2,2-trifluoroethyl)benzene (10), and 1-(1-Hydroxy-2,2,2-trifluoroethyl)-4-(formyl)benzene (11) - A solution of terephthaldicarboxaldehyde (2.63g, 19.61mmol) in anhydrous THF (50 ml) was stirred and cooled to 0ºC under an atmosphere of nitrogen. CF_3-TMS (5.58g, 39.22mmol) was added, and then tetrabutylammonium fluoride (0.3ml of 1.0M solution in THF) was added via syringe. The resulting yellow

solution was left to warm to room temperature for 13 h. Then ice (15ml) was added,

followed by hydrochloric acid (50 mL, 0.5M). Ether extraction followed by drying

($MgSO_4$) and rotary evaporation afforded a pale yellow solid shown by NMR to contain

10 and **11** in a 4:3 ratio.

1-(1-Hydroxy-2,2,2-trifluoroethyl)-4-(formyl)benzene (11) -

(R_f 0.70 1/1 ethyl acetate/chloroform) ^{1}H NMR δ 10.04 (s, 1H), 7.94 (d, J= 8.4 Hz, 2H),

7.75 (d, J= 8.4 Hz, 2H), 6.11 (d, J= 5.4 Hz, 1H), 5.36 (m, 1H); ^{19}F NMR δ −77.1 (d, J=

6.6 Hz). The crude reaction mixture of terephthaldicarboxaldehyde and (10) was

dissolved in anhydrous ether (15ml) and added dropwise to a stirred, cooled (0ºC)

solution of lithium aluminum hydride (1.00g, 26.35 mmol) in anhydrous ether (20 mL)

under an atmosphere of dry nitrogen. The mixture was allowed to warm to room

temperature over a period of 3 h. Then ice (20 mL) was added, along with sulphuric acid

(8 mL of 40% solution). After stirring for 1 h, ether extraction followed by drying

($MgSO_4$) and rotary evaporation gave a white solid that upon column chromatography

yielded **10** (R_f 0.80, 1/1 ethyl acetate/chloroform) and **12** (R_f 0.46, 1/1 ethyl

acetate/chloroform).

1,4-Bis-(1-hydroxy-2,2,2-trifluoroethyl)benzene (10) - (2.58 g, 48%) Mp = 116-118ºC.

(^{1}H NMR ($CDCl_3$/d_6-acetone 1/1) δ 7.53 (s, 4H), 5.91 (d, 2H), 5.07 and 5.05

(diastereomer) (m, 2H); ^{13}C NMR ($CDCl_3$/d_6-acetone 1/1) δ 71.7 and 71.6 (diastereomer)

(q, J= 31.5 Hz), 124.2 (q, J= 281.7 Hz), 127.2, 135.6; ^{19}F NMR δ –77.0 (d, J= 6.6 Hz);

MS (EI[+]) m/z 274 (15) [M[+]], 205 (1 0 0).

1-(1-Hydroxy-2,2,2-trifluoroethyl)-4-(hydroxymethyl)benzene (12) - (1.45 g, 36%).

Mp = 92-94ºC. ^{1}H NMR (CDCl$_3$/d$_6$-acetone 1/1) δ 7.47 (d, J= 8.0 Hz, 2H), 7.40 (d, J=8.0

Hz, 2H), 5.67 (d, J= 5.4 Hz, 1H), 5.03 (m, 1H), 4.78 (d, J= 5.7 Hz, 2H), 4.17 (t, J= 5.7

Hz, 1H); ^{13}C NMR (CDCl$_3$/d$_6$-acetone 1/1) δ 141.9, 133.3, 126.8, 125.8, 124.1 (q, J=

282.0 Hz), 71.3 (q, J= 31.2 Hz) 63.4; ^{19}F NMR δ –77.1 (d, J= 6.6 Hz); MS (EI[+]) *m/z* 206

(41) [M[+]], 137 (1 0 0).

1-(1-Chloro-2,2,2-trifluoroethyl)-4-(chloromethyl)benzene (13) - Diol **12** (20.00 g,

97.96 mmol) was dissolved in pyridine (23 mL, 0.28 mol) at room temperature under an

atmosphere of dry nitrogen. Thionyl chloride (34 mL, 0.47 mol) was added via syringe,

and the mixture was brought to reflux for a period of 24 h. The excess pyridine and

thionyl chloride were removed by distillation, and the resulting brown sludge was

absorbed on an equal volume of silica gel and column chromatography produced **13** (R_f

0.45, 19/1 hexane/ether) (14.22 g, 60%). Pale yellow oil. ^{1}H NMR δ 7.50 (d, J= 8.0 Hz,

2H), 7.45 (d, J= 8.0 Hz, 2H), 5.12 (q, J= 6.8 Hz, 1H), 4.61 (s, 2H); ^{13}C NMR δ 138.2,

131.0, 127.9, 127.7, 122.1 (q, J= 278.9 Hz), 57.1 (q, J= 34.3 Hz), 44.2; ^{19}F NMR δ –77.1

(d, J= 6.6 Hz); MS (EI[+]) *m/z* 242 (26) [M[+]], 207 (1 0 0).

1,4-Bis-(1-chloro-2,2,2-trifluoroethyl)benzene (14) - Using the same scale and procedure for **13**, diol **10** was converted to **14** (R_f 0.46, 19/1 hexane/ether) (65%). Pale yellow oil. ^{1}H NMR δ 7.56 (s, 4H), 5.15 (q, J= 6.7 Hz, 2H); ^{13}C NMR δ 134.1, 129.2, 123.3 (q, J= 278.5 Hz), 58.13 and 58.11 (diastereomer) (q, J= 34.6 Hz); ^{19}F NMR δ – 73.1 (d, J= 6.7 Hz); MS (EI^{+}) m/z 310 (35) [M^{+}], 241 (1 0 0); HRMS (CI^{+}) calculated for $C_{10}H_6Cl_2F_6$[MH]$^{+}$ 310.98290, found 310.9841.

1-(1-Chloro-2,2,2-trifluoroethyl)-4-[ethoxy(thiocarbonyl)thiomethyl]benzene (15) - Potassium *O*-ethyl xanthic acid salt (1.04 g, 6.49 mmol) was added to a solution of **13** (1.00 g, 4.33 mmol) in methanol (20 mL), and stirred at room temperature overnight. Then saturated NaCl solution (20 mL) was added along with dichloromethane (20 mL). After stirring for 25 min, extraction with dichloromethane, followed by drying (MgSO$_4$) and rotary evaporation and column chromatography (R_f 0.39, 3/2 hexane/dichloromethane) gave **15** (1.22g, 86%) colorless oil. ^{1}H NMR δ 7.42 (d, J= 8.4 Hz, 2H), 7.37 (d, J= 8.4 Hz, 2H), 5.11(q, J= 6.9 Hz, 1H), 4.63 (q, J= 7.2 Hz, 2H), 4.36 (s, 2H), 1.39 (t, J= 7.2 Hz, 3H); ^{13}C NMR δ 212.6, 137.1, 130.1, 128.2, 127.7, 122.1 (q, J= 278.9 Hz), 69.2, 57.2 (q, J= 34.3 Hz), 38.6, 12.7; ^{19}F NMR δ–73.1 (d, J= 6.9 Hz); HRMS (CI^{+}) calculated for $C_{12}H_{12}OF_3ClS_2$ 327.99702, found 327.9981.

1,4-Bis-[1-(methylthiocarbonyloxy-2,2,2-trifluoroethyl]benzene (16) - Using the same scale and procedure as for **17**, diol **10** gave **16** (R_f 0.50, 1/1 hexane/ether) (83%). Mp = 70-74°C. ^{1}H NMR δ 7.53 (s, 4H), 6.96 (q, J= 6.6 Hz, 2H), 2.62 (s, 6H); ^{13}C NMR δ 213.61 and 213.57 diastereomer, 132.3, 128.6, 122.6 (q, J= 280.6 Hz), 78.00 and 77.95 diastereomer (q, J= 33.2 Hz), 19.7; ^{19}F NMR δ –74.9 (d, J= 6.6 Hz); HRMS (CI[+]) calculated for $C_{14}H_{12}O_2F_6S_4$ 453.96244, found 453.9624.

1-[1-(Methylthio)thiocarbonyloxy-2,2,2-trifluoroethyl]-4-[methylthio(thiocarbonyl)oxymethyl]benzene (17) - Under an atmosphere of dry nitrogen, a mineral oil dispersion of sodium hydride (0.32 g of 60 wt.%, 7.88 mmol) was dissolved in anhydrous THF (10 mL) at room temperature. A solution of **12** (0.65 g, 3.15 mmol) in THF (10 mL) was added drop wise to the stirred solution, and after 60 min carbon disulphide (1.22 g, 15.75 mmol) was added via syringe. The mixture was stirred at room temperature for 1 h and then methyl iodide (2.23 g, 15.75 mmol) was added via syringe and the reaction was left to stir overnight. Afterwards ice/water (20 mL) was added, followed by ether extraction. The ether layers were combined, dried ($MgSO_4$) and rotary evaporated to yield a solid residue that upon column chromatography (R_f 0.40, 9/1 hexane/ether) afforded **(17)** (0.98 g, 81%). Colorless oil. ^{1}H NMR δ 7.49 (d, J= 8.0 Hz, 2H), 7.44 (d, J= 8.0 Hz, 2H), 6.89 (q, J= 6.9 Hz, 1H), 5.63 (s, 2H), 2.60 (s, 3H), 2.59 (s, 3H); ^{13}C NMR δ 215.3, 213.5, 136.6, 130.6, 128.5, 128.4, 122.6 (q, J= 280.3 Hz), 78.3 (q, J= 33.2 Hz), 74.0, 19.6, 19.2; ^{19}F NMR δ –75.0 (d, J= 6.9 Hz); MS (CI[+]) m/z 386 (70) [M[+]], 279 (1 0 0); HRMS (CI[+]) calculated for $C_{13}H_{13}O_2F_3S_4$ 385.97505, found 385.9742.

1-(1-Chloro-2,2,2-trifluoroethyl)-4-[(*n*-octylsulfinyl)methyl]benzene (18) - *n*-Octane

thiol (0.95 g, 6.49 mmol) was stirred with sodium *t*-butoxide (0.62 g, 6.49mmol) in

methanol (50 mL) for 30 min at room temperature, and then a solution of **13** (1.00g, 4.33

mmol in methanol (10 mL) was added. After 1h at room temperature, tellurium dioxide

(35 mg, 0.22 mmol) and hydrogen peroxide (1.26 mL of 35% solution) were added and

the reaction was stirred for another hour. Saturated sodium chloride solution (20 mL) was

added along with 20 ml of dichloromethane. After stirring for 1 h, dichloromethane

extraction followed by drying (MgSO$_4$) and rotary evaporation produced a solid residue

that upon column chromatography (R_f 0.53, 1/1 ether/chloroform) yielded **18** (1.42 g,

89%). Mp = 57-60ºC. ^{1}H NMR δ 7.47 (d, *J*= 7.8 Hz, 2H), 7.32 (d, *J*= 7.8 Hz, 2H), 5.11

(q, *J*= 6.6 Hz, 1H), 3.95 and 3.93 (diastereomer) (d, *J*= 13.5 Hz, 2H), 2.58 (t, *J*= 8.1 Hz,

2H), 1.76 9 (m, 2H), 1.40-1.24 (m, 10H), 0.85 (t, *J*= 5.1 Hz, 3H); ^{13}C NMR δ 131.2,

131.0, 129.2, 128.0, 122.1 (q, *J*= 278.6 Hz), 57.1 (q, *J*= 34.3 Hz), 56.5 and 56.4

(diastereomer), 50.33 and 50.29 (diastereomer), 30.6, 28.1, 27.9, 27.7, 21.5, 21.4, 13.0;

^{19}F NMR δ–73.1 (d, *J*= 6.6 Hz); HRMS (CI$^+$) calculated for C$_{17}$H$_{24}$OF$_3$ClS [MH]$^+$

369.12668, found 369.1269.

1-(1-Chloro-2,2,2-trifluoroethyl)-4-[(*n*-octylsulfonyl)methyl]benzene (19) - A solution

(5 mL) of **18** (0.18 g, 0.51 mmol) was cooled to 0ºC under an atmosphere of dry nitrogen,

and over a period of 15 min in a solution of *m*CPBA (0.88 g, 5.07 mmol) in

dichloromethane (15 mL) was added. The solution was warmed to room temperature and

stirred for an additional hour. Then sodium hydroxide (10 mL of 5% solution) was added,

followed by 30 mL of dichloromethane. Dichloromethane extraction, drying (MgSO$_4$)

and rotary evaporation produced a white solid residue that after column chromatography

(R_f 0.41, 2/1 ether/hexane) afforded **19** (0.19 g, 94%). Mp = 94-96ºC. ^{1}H NMR δ 7.51 (d,

J= 8.4 Hz, 2H), 7.43 (d, J= 8.4 Hz, 2H), 5.13 (q, J= 6.9 Hz, 1H), 4.21 (diastereomer) (d,

J= 13.5 Hz, 2 H), 2.58 (t, J= 8.1 Hz, 2H), 1.76 (m, 2H), 1.40-1.24 (m, 10H), 0.85 (t, J=

5.1 Hz, 3 H); ^{13}C NMR δ 131.2, 130.9, 129.2, 128.0, 122.0 (q, J= 278.6 Hz), 57.1 (q, J=

34.3 Hz), 56.5 and 56.4 (diastereomer), 50.33 and 50.29 (diastereomer), 30.6, 28.0, 27.9,

27.7, 21.5, 21.4, 13.0; ^{19}F NMR δ –73.1 (d, J= 6.9Hz); HRMS (CI[+]) calculated for

$C_{17}H_{24}O_2F_3ClS$ [MH][+] 385.1215, found 385.1203.

1-(1-*p*-Toluenesulfonyloxy-2,2,2-trifluoroethyl)-4-[(p-

toluenesulphonyloxy)methyl]benzene (20) - Under an atmosphere of dry nitrogen, a

mineral oil dispersion of sodium hydride (1.02 g of 60 wt.%., 25.49 mmol) was dissolved

in anhydrous THF (40mL) at room temperature. A solution of **12** (2.50 g, 12.14 mmol) in

THF (80 mL) was added dropwise to the stirred solution, and after 50 min a solution of

tosyl chloride (5.78 g, 30.35 mmol) in THF (40 mL) was added dropwise. The resulting

creamy yellow mixture was warmed to reflux overnight. After cooling to room

temperature, ice (25 mL) was added, and this was followed by ether extraction. The ether

layers were combined, dried (MgSO$_4$) and rotary evaporated to yield a pale yellow solid,

that upon chromatography (R_f 0.42, 2/1 ether/hexane) afforded **20** (5.49 g, 88%). Mp =

137-140ºC. ^{1}H NMR δ 7.75 (d, J= 8.1 Hz, 2H), 7.62 (d, J= 8.1 Hz, 2H), 7.31 (d, J= 8.1

Hz, 2H), 7.27 (d, J= 8.1Hz, 2 H), 7.24 (d, J= 8.1Hz, 2H), 7.19 (d, J= 8.1 Hz, 2H), 5.62 (q,

J= 6.3 Hz, 1H), 5.02 (s, 2H), 2.44 (s, 3H), 2.40 (s, 3H); ^{13}C NMR δ 145.5, 145.0, 135.5,

132.9, 132.6, 130.4, 129.8, 129.7, 128.4, 128.2, 127.8, 127.7, 121.9 (q, J= 280.5 Hz),

77.4 (q, J= 34.3 Hz), 70.8, 21.7, 21.6; ^{19}F NMR δ –76.7 (d, J= 6.3 Hz); HRMS (ESI)

calculated for $C_{23}H_{21}O_6F_3S_2$ [M + Na][+] 537.06294, found 537.0646.

When the above reaction was performed with 1.5 equivalents of sodium hydride, column

chromatography of the product mixture afforded **20**(R_f 0.42, 2/1 ether/hexane) (3.06 g,

49%) and 1-(1-*p*-toluenesulphonyloxy-2,2,2-trifluoroethyl)-4-(hydroxymethyl)benzene

21(R_f 0.59, ether) (1.40 g, 32%). Mp = 79-81ºC. ^{1}H NMR δ 7.54 (d, J= 7.6 Hz, 2H), 7.19

(s, 4H), 7.11 (d, J= 7.6 Hz, 2H), 5.55 (q, J= 6.0 Hz, 1H), 4.55 (s, 2H), 2.29 (s, 3H); [13]C

NMR δ 145.3, 143.1 132.8, 129.6 128.8, 128.1, 127.8, 126.8, 122.1, (q, J= 280.8 Hz),

77.7 (q, J= 34.0 Hz), 64.4, 21.6; ^{19}F NMR δ –76.0 (d, J= 6.0 Hz); MS (CI[+]) *m/z* 359 (41)

[M–H][+], 343 (1 0 0); HRMS (ESI) calculated for $C_{16}H_{15}O_4F_3S$ [M + Na][+] 383.05408,

found 383.0514.

1,4-Bis-(1-*p*-toluenesulphonyloxy-2,2,2-trifluoroethyl)benzene (22) - Using the same

scale and procedure as for **20** bis diol **10** was converted to **22** (R_f 0.47, 2/1 ether/hexane)

(83%). Mp = 205-207ºC. ^{1}H NMR δ 7.49 and 7.47 diastereomer (d, J= 8.4 Hz, 4H), 7.13

and 7.11 diastereomer (s, 4H), 7.09 and 7.08 diastereomer (d, J= 8.4 Hz, 4H), 5.57 and

5.55 diastereomer (q, J= 6.3 Hz, 2H) 2.28 (s, 6H); ^{13}C NMR δ 145.6, 132.57 and 132.52

diastereomer, 131.7 and 131.1 diastereomer, 129.63 and 129.61 diastereomer, 129.2,

127.72 and 127.67 diastereomer, 121.8 (q, J= 280.8 Hz), 77.4 and 77.3 diastereomer (q,

J= 34.0 Hz), 21.6; ^{19}F NMR δ –75.9 and –76.0 diastereomer (d, J= 6.3 Hz); MS (EI) m/z

582 (10) [M[+]], 91 (1 0 0); HRMS (ESI) calculated for $C_{24}H_{20}O_6F_6S_2$ [M + Na][+]

605.05032, found 605.0529.

1-(1-*p*-Toluenesulphonyloxy-2,2,2-trifluoroethyl)-4-

[ethoxy(thiocarbonyl)thiomethyl]benzene (23) - Potassium *O*-ethyl xanthic acid salt

(0.75 g, 4.69 mmol) was added to a solution of **20** (2.00 g, 3.89 mmol) in methanol (20

mL), and stirred at room temperature overnight. Then saturated NaCl solution (20 mL)

was added along with dichloromethane (20 mL). After stirring for 20 min, extraction with

dichloromethane, followed by drying (MgSO$_4$), rotary evaporation and column

chromatography (R_f 0.55, 1/1 ether/hexane) gave **23** (1.61 g, 89%). Mp = 67-68ºC. [1]H

NMR δ 7.56 (d, J= 8.1 Hz, 2H), 7.21 (s, 4H), 7.14 (d, J= 8.1 Hz, 2H), 5.64 (q, J= 6.3 Hz,

1H), 4.62 (q, J= 7.2 Hz, 2H), 4.29 (s, 2H), 2.35 (s, 3H), 1.38 (t, J= 7.2 Hz, 3H); ^{13}C NMR

δ 213.2, 145.3, 138.2, 132.6, 129.5, 129.0, 128.6, 128.1, 127.6, 122.0 (q, J= 280.6 Hz),

77.7 (q, J= 34.4 Hz), 70.2, 39.6, 21.5, 13.7; ^{19}F NMR δ –75.9 (d, J= 6.3 Hz); HRMS

(ESI) calculated for $C_{19}H_{19}O_4F_3S_3$ [M + Na][+] 487.02953, found 487.0274.

1-(1-*p*-Toluenesulphonyloxy-2,2,2-trifluoroethyl)-4-[(*n*-octylsulfinyl)methyl]benzene

(24) - *n*-Octane thiol (0.67 g, 4.55 mmol) was stirred with sodium *t*- butoxide (0.44 g,

4.55 mmol) in methanol (20mL) for 30 min at room temperature, and then a solution of

(20) (1.95 g, 3.79 mmol) in methanol (15 mL) was added. After stirring for 1 h at room

temperature, tellurium dioxide (3 mg, 0.18 mmol) and hydrogen peroxide (1.2 mL of 10 M solution, 11.37 mmol) were added and stirred for another hour. Saturated sodium chloride solution (20 mL) was added along with 20 mL of dichloromethane, and after stirring for 1 h, dichloromethane extraction followed by drying (MgSO$_4$) and rotary evaporation produced a solid residue that upon column chromatography (R_f 0.50, 1/1 ether/chloroform) yielded **24** (1.70 g, 89%). Mp = 95-97 ºC. ^{1}H NMR δ 7.64 and 7.63 (d, J= 8.1 Hz, 2H), 7.33 and 7.32 (d, J= 8.1 Hz, 2H), 7.24 and 7.23 (d, J= 8.1 Hz, 2H), 7.23 and 7.22 (d, J= 8.1 Hz, 2H), 5.63 and 5.61 (q, J= 6.3 Hz, 1H), 3.89 and 3.88 (s, 2H), 2.59 (t, J= 7.6 Hz, 2H), 2.39 (s, 3H) 1.77 (m, 2H), 1.40-1.20 (m, 10H), 0.86 (m, 3H); ^{13}C NMR δ 145.5 and 145.4 diastereomer, 132.80 and 132.77 diastereomer, 132.67 and 132.62 diastereomer, 130.2, 129.9 and 129.8 diastereomer, 129.7, 128.5, 127.8, 122.0 (q, J= 280.8 Hz), 77.5 and 77.4 diastereomer (q, J= 34.3 Hz), 57.83 and 57.79 diastereomer, 31.8, 31.0, 29.2, 28.9, 22.7, 21.8, 14.1; ^{19}F NMR δ −75.8 (d, J= 6.3 Hz); HRMS (ESI) calculated for C$_{24}$H$_{31}$O$_4$F$_3$S$_2$ [M + Na]$^+$ 527.15136, found 527.1498.

1-(1-*p*-Toluenesulphonyloxy-2,2,2-trifluoroethyl)-4-[(n-octylsulfonyl)methyl]benzene (25) - A dichloromethane solution (5 mL) of **24** (0.43 g, 0.85 mmol) was cooled to 0ºC under an atmosphere of dry nitrogen, and over a period of 15 min a solution of *m*CPBA (0.15g, 0.85 mmol) in dichloromethane (15 mL) was added. The solution was warmed to room temperature and stirred for an additional hour. Then sodium hydroxide (5 mL of 5%) solution was added followed by 30 mL of dichloromethane. Dichloromethane extraction, drying (MgSO$_4$) and rotary evaporation produced a solid residue that after

column chromatography (R_f 0.38, 3/1 ether/hexane) afforded **25** (0.39g, 89%). Mp = 93-

95°C. ^{1}H NMR δ 7.66 (d, *J*= 8.4 Hz, 2H), 7.38 (s, 4H), 7.24 (d, *J*= 8.4 Hz, 2H), 5.68 (q,

J= 6.3 Hz, 1H), 4.18 (s, 2H), 2.86 (t, *J*= 7.8 Hz, 2H), 2.42 (s, 3H), 1.82 (m, 2H), 1.54-

1.10 (m, 10 H), 0.87 (m, 3H); ^{13}C NMR δ 145.6, 132.7, 130.9, 130.6, 130.1, 129.8, 128.6,

127.8, 122.0 (q, *J*= 280.8 Hz), 77.4, (q, *J*= 34.3 Hz), 58.7, 31.7, 29.1, 29.0, 28.5, 22.7,

22.0, 14.1; ^{19}F NMR δ –75.9 (d, *J*= 6.3 Hz); HRMS (ESI) calculated for $C_{24}H_{31}O_5F_3S_2$

$[M + Na]^+$ 543.14627, found 543.1448.

1-(1-Pyridinium-2,2,2-trifluoroethyl)-4-[(pyridinium)methyl]benzene-

bis(trifluoromethansulfonate) (27) - Under an atmosphere of dry nitrogen a solution of

diol **12** (0.21 g, 1.03 mmol) in pyridine (3 mL) was cooled to 0°C. After stirring for 1 h at

room temperature, triflic anhydride (1.67 g, 2.5 mmol) was added via syringe. The

resulting bright red solution was stirred and allowed to warm to room temperature over a

period of 4 h. Then ice (20 mL) was added to the reaction. The solution was adjusted to

neutral pH and the aqueous layer was extracted with ether. The aqueous layer was

evaporated, was shown to contain **27** in 78% yield (based on a ^{19}F NMR yield versus a

known amount of added trifluoroethanoic acid). The purity was enhanced by several

recrystallizations from 2:1 water/acetone. Mp > 275°C. ^{1}H NMR (D_2O:acetone-d_6 1/1) δ

8.90 (d, *J*= 6.3 Hz, 2H), 8.78 (d, *J*= 6.0 Hz, 2H), 8.60 (t, *J*= 6.6 Hz, 1H), 8.45 (t, *J*= 6.6

Hz, 1H), 8.06 (t, *J*= 7.2 Hz, 2H), 7.96 (t, *J*= 6.9 Hz, 2H), 7.65 (t, *J*= 7.8 Hz, 2H), 7.50 (t,

J= 7.8 Hz, 2H), 7.00 (q, *J*= 7.2 Hz, 1H), 5.78 (s, 2H); ^{19}F NMR (D_2O:acetone-d_6 1/1) δ –

69.1 (d, J= 7.2 Hz, 3F), −77.5 (s, 6F); MS (APCI:AP$^+$) m/z 479 (1 0 0)

[$C_{19}H_{17}F_3N_2$$^{2+}$ 2CF$_3$SO$_3$$^-$]; (AP$^-$) 149 (1 0 0) [CF$_3SO_3$$^-$].

1,4-Bis-(1-pyridinium-2,2,2-trifluoroethyl)benzene-bis(trifluoromethansulfonate)

(26) - Using the same scale and procedure as for **27**, diol **10** was converted to **26** (85%

yield based on a ^{19}F NMR yield versus a known amount of added trifluoroethanoic acid).

Mp > 275ºC. ^{1}H NMR (D$_2$O: acetone-d$_6$ 1/1) δ 9.25 (d, J= 6.0 Hz, 4H), 8.88 (t, J= 6.6 Hz,

2H), 8.36 (t, J= 6.9 Hz, 4H), 8.05 (s, 4H), 7.45 (q, J= 6.9 Hz, 2H); ^{13}C NMR

(D$_2$O:acetone-d$_6$ 1/1) δ 149.5, 145.3, 131.5, 130.5, 129.8, 122.7 (q, J= 283.4 Hz), 120.4

(q, J= 280.6 Hz), 71.8 (q, J= 32.7 Hz); ^{19}F NMR (D$_2$O:acetone-d$_6$ 1/1) δ −70.3 (d, J= 6.9

Hz, 6F), −79.5 (s, 6F); MS (APCI:AP$^+$) m/z 547 (31) [$C_{20}H_{16}F_6N_2$$^{2+}$ 2 CF$_3$SO$_3$$^-$], 398

(1 0 0); (AP$^-$) 149 (1 0 0)[CF$_3$SO$_3$$^-$].

References

[1]P. Bernier. Handbook of Conducting Polymers. Ed. Terje A. Skotheim. Vol 2. New York: Academic Press, 1984; 325, 331, 336-337.

[2]G. Natta, G. Mazzanti, P. Corrandi, Atti. Accad. Naz. Lincei Rend. Cl. Sci. Fis. Mat. Nat., 8:3, 1958.

[3]A. Heeger, A. MacDiarmid, H. Shirakawa, Nobel Lectures, 1996-2000, World Scientific Publishing Co., Singapore, 2003.

[4] J.C.W. Chien. Polyacetylene: Chemistry, Physics, and Material Science. Orlando: Academic Press, 1984; 325, 331, 336-337.

[5]H. Mizes, E.M. Conwell, Synthetic Metals, 1995, Volume 68, Issue 2, 145-151.

[6]R. Farchiono, G. Grosso. Organic Electronic Materials Conjugated Polymers and Low Molecular Weight Organic Solids. Berlin: Springer, 2001; 128, 134, and 136.

[7]J. Segura, Acta Polym., 1998, 49, 319-344.

[8]R. Friend, R. Gymer, A. Holmes, J. Burroughes, R.. Marks, C. Taliani, D.D.C. Bradley, D.A. Dos Santos, J.Bredas, Loglund, W.R. Salaneck, Nature, 1999, Vol 397, 121-128.

[9]S. Moratti, R. Cervini, A. Holmes, D. Baignet, R. Friend, N. Greenham, J. Gruner, P.J. Hamer, Synthetic Metals, 1995, 71, 2117-2120.

[10]S. Lo, L. Palsson, M. Kiliziraki, P. Burn, I. Samuel, J. Mater.Chem., 2001, 11, 2228-2231.

[11]A. Greiner, Polym. Adv. Technol., 1998, 9, 371-389.

[12]L. Lutsen, I. Duyssens, H. Penxten, D. Vanderzande, Synthetic Metals, 2003, 139, 589-592.

[13]C. Xue, F. Luo, J. Org. Chem., 2003, 68, 4417-4421.

[14]H.C. Lin, C. Tsai, G. Huang, J. Lin, Journal of Polymer Science, 2006, 44, 783-800.

[15]G. Samal, A. Tirpathi, A. Biswas, S. Singh, Y. Mohapatra, Synthetic Metals, 2005, 155, 344-348.

[16]H. Tilmann, H. Horhold, Synthetic Metals, 1999, 101, 138-139.

[17]Y. Li, Y. Cao, D. Wang, G. Yu, A. Heeger, Synthetic Metals, 1999, 99, 243-248.

[18]G. Samal, A. Tirpathi, A. Biswas, S. Singh, Y. Mohapatra, Synthetic Metals, 2005, 155, 303-305.

[19]C. Vijila, B. Balakrisnan, C. Huang, Z. Chen, C. Zhen, M. Auch, S. Chua, Chemical Physics Letters, 2005, 414, 393-397.

[20]A. Lux, A. Holmes, R. Cervini, J.Davies, S. Moratti, J. Gruner, F. Cacialli, R. Friend, Synthetic Metals, 1997, 84, 293-294.

[21]S. Gillissen, M. Kesters, T. Johansson, M. Theander, M. Andersson, O. Inganas, L. Lutsen, D. Vanderzande, Macromolecules, 2001, 34, 7294-7299.

[22]H. Gilch., Journal of Polymer Science: Part A-1, 1966, 4, 1337-1349.

[23]A. Issaris, D. Vanderzande, P. Adriaensans, J. Gelan, Macromolecules, 1998, 31, 4426-4431.

[24]B. Cho, Prog. Polym. Sci., 2002, 27, 307-355.

[25]P.Adriaensens, M. Van Der Borght, L. Hontis, A. Issaris, A. van Breeman, M. de Kok, D. Vanderzande, J. Gelan. Polymer. 2000, 41, 7003-7009.

[26]F. Louwet, D. Vanderzande, J. Gelan, Synthetic Metals, 1995, 69, 509-510.

[27]M. Mitsuyoshi , H. Tachibanam, T. Nakamura. Organic Conductors Fundamentals and Applications. Ed. Jean-Pierre Farges. New York, NY: Dekker Inc., 1994.

[28]A.J.Roche, A. Loyle, J.P. Pinto, Journal of Fluorine Chemistry, 2004, 125, 1473-1480.

[29]M. McClinton, D. McClinton. Tetrahedron, 1992, 48(32), 6555-6666.

[30]T. Umemoto, K. Adachi, S. Ishihara. J. Org. Chem., 2007, 72, 6905-6917.

[31]I. Ruppert. Journal of Fluorine Chemistry, 1985, 29(1-2), 98.

[32]G. Surya Prakash, J. Hu, Acc. Chem. Res., 2007, 40(10), 921-930.

[33]G. Surya Prakash, A. Yudin, Chem. Rev., 1997, 97, 757-786.

[34]D. Adams, J. Clark, L. Hansen, V. Sanders, S. Tavener, Journal of Fluorine Chemistry, 1998, 92, 123-125.

[35]S. Mizuta, N. Shibata, M. Hibino, S. Nagano, S. Nakamura, T.Toru, Tetrahedron, 2007, 63(35), 8521-8528.

[36]J. Romanski, G. Mloston, Arkivoc, 2007, Vol. 6, 179-187.

[37]A.D. Allen, I.C. Ambidge, C. Che, H. Michael, R.J. Muir, T. Tidwell, J. Am. Chem. Soc., 1983, 105, 2343-2350.

[38]Y. Gong, K. Kato, Synlett., 2002, 3, 431-434.

[39]L.G. Wade Jr., Organic Chemistry 5th Edition, New Jersey: Pearson Education Inc., 2003; 174-177.

[40]A.J. Roche, Magnetic Resonance in Chemistry, 2004, 42, 944-949.

[41]Gaussian 03, Revision C.02, M. J. Frisch,; G. W Trucks; H. B Schlegel; G. E Scuseria; M. A. Robb; J. R Cheeseman; J. A. Montgomery, Jr.; T.Vreven; K. N. Kudin; J. C. Burant; J. M. Millam; S. S. Iyengar; J. Tomasi; V. Barone; B. Mennucci; M. Cossi; G. Scalmani; N. Rega; G. A. Petersson; H. Nakatsuji; M. Hada; M. Ehara; K. Toyota; R. Fukuda; J. Hasegawa; M. Ishida; T. Nakajima; Y. Honda; O. Kitao; H.Nakai; M. Klene; X. Li; J. E. Knox; H. P. Hratchian; J. B. Cross; V. Bakken; C. Adamo; J. Jaramillo; R. Gomperts; R. E. Stratmann; O. Yazyev; A. J. Austin; R. Cammi; C. Pomelli; J. W. Ochterski; P. Y. Ayala; K. Morokuma; G. A. Voth; P. Salvador; J. J. Dannenberg; V. G. Zakrzewski; S. Dapprich; A. D. Daniels; M. C. Strain; O. Farkas; D. K. Malick; A. D. Rabuck; K. Raghavachari; J. B. Foresman; J. V. Ortiz; Q. Cui; A. G. Baboul; S. Clifford; J. Cioslowski; B. B. Stefanov; G. Liu; A. Liashenko; P. Piskorz; I. Komaromi; R. L. Martin; D. J. Fox; T. Keith; M. A. Al-Laham; C. Y. Peng; A. Nanayakkara; M. Challacombe; P. M. W. Gill; B. Johnson; W. Chen; M. W. Wong; C. Gonzalez; and J. A. Pople; Gaussian, Inc., Wallingford CT, 2004.

[42]A. Becke, J.Chem.Phys, 1993, 98, 5648-5652.

[43]P. Stephens, F.J. Devlin, C.F. Chabalowski, M.J. Frisch, J.Phys.Chem, 1994, 98, 11623-11627.